T.R.
ONDOKUZ MAYIS UNIVERSITY
INSTITUTE OF GRADUATE STUDIES
DEPARTMENT OF SOIL SCIENCE AND PLANT NUTRITION

BIOCHAR-BASED NANOCOMPOSITES FOR REMEDIATION OF SOIL AND WATER CONTAMINATED WITH HEAVY METALS

Master's Thesis

Muhammad Tukur BAYERO

Supervısor
Dr. Mahmoud MAZARJI

II. Supervisor

Associate.Prof. Svetlana SUSHKOVA

Prof.Dr. Tatiana MINKINA

Prof.Dr. Coşkun GÜLSER

SAMSUN
2022

T.R.
ONDOKUZ MAYIS UNIVERSITY
INSTITUTE OF GRADUATE STUDIES
DEPARTMENT OF SOIL SCIENCE AND PLANT NUTRITION

BIOCHAR-BASED NANOCOMPOSITES FOR REMEDIATION OF SOIL AND WATER CONTAMINATED WITH HEAVY METALS

Master's Thesis

Muhammad Tukur BAYERO

Supervisor

Dr. Mahmoud MAZARJI

II. Supervisor

Associate.Prof. Svetlana SUSHKOVA

Prof. Dr. Tatiana Minkina

Prof. Dr. Coşkun GÜLSER

This thesis was supported by the European Union project of Erasmus Mundus Master in Soil Science (emiSS) with project number 610528-EPP-1-2019-1-TR-EPPKA1-JMD-MOB)

SAMSUN
2022

ACCEPTANCE AND APPROVAL OF THE THESIS

The study entitled **"BIOCHAR-BASED NANOCOMPOSITES FOR REMEDIATION OF SOIL AND WATER CONTAMINATED WITH HEAVY METALS "** prepared by **Muhammad Tukur BAYERO**, and supervised by **Dr. Mahmoud MAZARJI, Associate.Prof. Svetlana SUSHKOVA, Prof.Dr. Tatiana MINKINA, and Prof. Dr. Coşkun GÜLSER**, was found successful and unanimously accepted by committee members as Master thesis, following the examination on the date 6.7.2022 .

	Title Name SURNAME University Department	**Signature**	**Final Decision**
Chairman	Dr. Mahmoud MAZARJI Southern Federal University Department of Soil Science and Land Resources Evaluation		☒ Accept ☐ Reject
Member	Prof. Dr. Coşkun GÜLSER Ondokuz Mayıs University Department of Soil Science and Plant Nutrition		☒ Accept ☐ Reject
Member	Prof. Dr. Orhan DENGIZ Ondokuz Mayıs University Department of Soil Science and Plant Nutrition		☒ Accept ☐ Reject
Member	Prof. Dr. Rıdvan KIZILKAYA Ondokuz Mayıs University Department of Soil Science and Plant Nutrition		☒ Accept ☐ Reject
Member	Assoc. Prof. Dr. Svetlana SUSHKOVA Southern Federal University Department of Soil Science and Land Resources Evaluation		☒ Accept ☐ Reject

This thesis has been approved by the committee members that already stated above and determined by the Institute Executive Board.

.

APPOVAL
… / … / …
Prof. Dr. Ali BOLAT
Head of Institute of Graduate Studies

DECLARATION OF COMPLIANCE WITH SCIENTIFIC ETHIC

I hereby declare and undertake that I complied with scientific ethics and academic rules in all stages of my Master's Thesis , that I have referred to each quotation that I use directly or indirectly in the study and that the works I have used consist of those shown in the sources, that it was written in accordance with the institute writing guide and that the situations stated in the article 3, section 9 of the Regulation for TÜBİTAK Research and Publication Ethics Board were not violated.

Is Ethics Committee Necessary?

Yes ☐ (If it necessary, please add appendices.)

No ☒

06 /07 / 2022
Muhammad Tukur BAYERO

DECLARATION OF THE THESIS STUDY ORIGINALITY REPORT

Thesis Title : BIOCHAR-BASED NANOCOMPOSITES FOR REMEDIATION OF SOIL AND WATER CONTAMINATED WITH HEAVY METALS

As a result of the originality report taken by me from the plagiarism detection program on 17/06 /2022 for the thesis titled above;

Similarity ratio : % 18

Single resource rate : % 2 has been released.

Signature
06 /07 / 2022
Prof. Dr. Coşkun GÜLSER

ÖZET

AĞIR METALLERLE KİRLENMİŞ TOPRAK VE SUYUN İYİLEŞTİRİLMESİ İÇİN BİYOKAR BAZLI NANOKOMPOZİTLER

Muhammad Tukur BAYERO
Ondokuz Mayıs Üniversitesi
Lisansüstü Eğitim Enstitüsü
Toprak Bilimi ve Bitki Besleme Bölümü
Erasmus Mundus Toprak Bilimi Yüksek Lisans (emiSS)
Yüksek Lisans, Haziran/2022
Danışman: Dr. Öğr. Üyesi Mahmoud MAZARJI

Gerçek kontamine toprakta potansiyel olarak toksik elementlerin mobilizasyonu ve taşınması çevre için önemli riskler oluşturur. Bu dünya çapındaki zorluğu çözmek için özel bir çözüm üretilmelidir. Bu çalışmada, ilk kez Fe bazlı metal-organik çerçeve (MIL-101(Fe)) biochar ile birleştirildi ve gerçek yüksek derecede kirlenmiş teknojenik toprakta dinamik liç kolonu deneylerinde bir değişiklik olarak uygulandı. Bu kapsamda, Materials Institute Lavoisier (MIL-101(Fe)) kompozitleri, metal-organik çerçeveler (MOF'ler) olarak solvotermal sentez prosedürü ile biyokömür yüzeyine başarıyla monte edildi. MIL-101(Fe) ve RBC-MIL dahil olmak üzere hazırlanan tüm numuneleri karakterize etmek için X-ışını kırınımı (XRD), Fourier-dönüşümlü kızılötesi spektroskopisi (FTIR), taramalı elektron mikroskobu (SEM) ve transmisyon elektron mikroskobu (TEM) kullanıldı. 101(Fe) kompozit. RBC-MIL 101(Fe) varlığında sızıntı suyundaki Cu içeriğini modellemek için tepki yüzey metodolojisi (RSM) kullanıldı. İkinci dereceden modeller, RBC-MIL 101(Fe) varlığında sorbent-toprak kütle oranı (x_1) ve süzme süresinin (x_2) bağımsız parametreleri dikkate alınarak oluşturulmuştur. Cu immobilizasyonunun etkinliğinin toprakta 3% RBC-MIL 101(Fe) varlığında ve minimum 0,2 mg L^{-1} konsantrasyonu ile 2 günlük bir süzme süresinde arttığı gözlendi. Kimyasal fraksiyonlama sonuçlarına göre, RBC-MIL101(Fe), Cu'nun asitte çözünür fraksiyonunu, onu artık fraksiyona yerleştirerek önemli ölçüde azaltmıştır. Genel olarak, bulgularımız MOF bazlı biyokömür kompozitlerinin gerçek kirlenmiş toprak restorasyonunda gelişmiş değişiklikler olarak kullanılmasının yolunu açıyor.

Anahtar Sözcükler: Nanomalzemeler, Metal-organik çerçeveler, Bakır, Gerçek kirlenmiş toprak, liç, immobilizasyon

ABSTRACT

BIOCHAR-BASED NANOCOMPOSITES FOR REMEDIATION OF SOIL AND WATER CONTAMINATED WITH HEAVY METALS

Muhammad Tukur BAYERO
Ondokuz Mayıs University
Institute of Graduate Studies
Department of Soil Science and Plant Nutrition
Erasmus Mundus Master in Soil Science (emiSS) Program
Master, June/2022
Supervisor: Assist. Prof. Dr. Mahmoud MAZARJI

The mobilization and transport of potentially toxic elements in real-contaminated soil pose significant risks to the environment. To solve this worldwide challenge, a tailored solution must be produced. In this study, for the first time, Iron-based metal-organic framework (MIL-101(Fe)) was composited with biochar and implemented as an amendment on dynamic leaching column experiments in real highly contaminated technogenic soil. In this context, Materials Institute Lavoisier (MIL-101(Fe)) was successfully mounted on biochar surface by solvothermal synthesis procedure. X-ray diffraction (XRD), scanning electron microscopy (SEM) Fourier-transform infrared spectroscopy (FTIR), and transmission electron microscopy (TEM) were employed for characterizing all prepared samples including MIL-101(Fe), and RBC-MIL 101(Fe) composite. Response surface methodology (RSM) was utilized to model Cu contents in the leachate in the presence of RBC-MIL 101(Fe). The quadratic models were built considering independent parameters of sorbent-to-soil mass ratio (x_1) and leaching time (x_2) in the presence of RBC-MIL 101(Fe). The effectiveness of Cu immobilization was observed to improve in the presence of 3% RBC-MIL 101(Fe) in the soil and a leaching period of 2 days with the minimum concentration of 0.2 mg L^{-1}. According to the chemical fractionation results, RBC-MIL101(Fe) remarkably decreased the acid soluble fraction of Cu by deploying it in the residual fraction. Overall, our findings pave the way for MOF-based biochar composites to be used as advanced amendments in real contaminated soil restoration.

Keywords: Nanomaterials, Metal-organic frameworks, Copper, Real contaminated soil, leaching, immobilization

ACKNOWLEDGEMENT

I wish to express my gratitude for the fellowship support of the European Union Project of Erasmus Mundus Master in Soil Science (emiSS) (No. 610528-EPP-1-2019-1-TR-EPPKA1-JMD-MOB).

Muhammad Tukur BAYERO

CONTENTS

ABBREVIATION OF TERMS

ANOVA	: Analysis of variance
CCD	: Central Composite Design
Cu	: Copper
MIL	: Materials of Institute Lavoisier
MOF	: Metal-organic Frameworks
PTE	: Potentially Toxic Elements
RBC	: Rice Husk Biochar
RSM	: Response Surface Methodology
ZIF	: Zeolitic Imidazolate Frameworks

FIGURES LEGENDS

TABLES LEGENDS

1. INTRODUCTION

1.1. Background

Soils offer basic human needs from food to clean water, and air, as well as acting as a key drivers for biodiversity. Soil sustainability is beyond the farmers and land users but highly dependent on government decisions on grants, subsidies and capacity building (J. Huang et al., 2018). Soil pollution caused by numerous heavy metals or potentially toxic elements (PTE) is a global environmental issue that has yet to find a long-term solution (Qian, Liang, Zhang, Huang, & Diao, 2022a). Heavy metal ions such as copper (Cu), zinc (Zn), arsenic (As), mercury (Hg), cadmium (Cd), lead (Pb), chromium (Cr), and other heavy metals have been accumulating in the soil due to the discharge of various wastes from industrial activities, mining operations, municipal areas, agricultural processes, and other anthropogenic sources (Fan et al., 2020a; Qian et al., 2022a; Yutong, Qing, & Shenggao, 2016). As a result, the risk of mobilization and migration of heavy metals entering the food chain keeps rising, posing a major health threat (J. Huang et al., 2018; J. Liu, Liu, Liu, Liu, & Zhang, 2018; Yutong et al., 2016). Cu is one of the pollutants that must be removed at concentrations higher than the threshold level of 20 - 30 mg/kg, depending on the region, during soil remediation to prevent mobilization and migration.(Lado, Hengl, & Reuter, 2008).

Effective soil restoration methods have evolved as a vital component in guaranteeing the long-term viability of soils. However, most techniques are expensive, take a long time to remove, and may cause secondary contamination in the soil (Gholizadeh & Hu, 2021a). Chemical treatments such as chemical precipitation, chemical fixation, and chemical leaching are examples of chemical methods.(Irshad & Mukhtar, 2020), and separation via electrokinetics (Kim, Jeong, Lee, Yun, & Jo, 2021) require high amount of chemicals. Biological methods of remediation like bioremediation (Wu et al., 2020) and phytoremediation which utilizes plants (Sarwar et al., 2017) are considered cheap and environmentally friendly. However, these methods are complex in design and slow in operation. Bioremediation employs uses both bacteria and fungi which are within the soil (Bano et al., 2018), which is complex to implement since these micro oragnisms thrive in a specific condition. Phytoremediation, on the other hand, employs specialized plant species to remove heavy metals. (Hayyat et al., 2016; Wan, Lei, & Chen, 2016). Despite its ease of use, treating complicated polluted areas with more than one heavy metal is slow and tedious

with this technique. (Gholizadeh & Hu, 2021b).

Biochar is a carbon containing porous material made by pyrolyzing biomass feedstocks at temperatures usually between 300 and 700°C depending on the application is a well established amendment for heavy metals polluted soils restoration (H. Huang et al., 2021). These biochars are used as either soil amendments for agriculture or for environmental remediation (Chausali, Saxena, & Prasad, 2021). Biochar and nanomaterials have both benefited greatly from the development of biochar-based composites. (Zhao et al., 2021). The resultant composites' functional groups, pore properties, and ease of separation are frequently much improved (Liang et al., 2021; Mandal et al., 2021). The addition of nanoparticles to biochar increases its potential for heavy metal immobilization, transforming the bionanocomposite into an effective heavy metal sorbent in soils (Arabyarmohammadi et al., 2018; Lyu et al., 2018; Mandal, Pu, Shangguan, et al., 2020)

By utilizing nanoscale materials, emerging nanotechnology technologies such as nano-enabled metal-organic frameworks (MOFs) received a lot of interest in recent decades in environmental matrices such as wastewater (S. Zhang et al., 2021a). MOFs are a revolutionary type of organic-inorganic hybrid crystalline porous material generated by strong covalent/coordination interactions between clusters of organic ligands and metal ions (S. Liu et al., 2020). Additionally, processes such as photocatalysis, fenton-like, radical sulfate oxidation and, especially adsorption have seen huge MOF applications (Figure 1.1) (Bayero et al., 2021). In this study, we aim to produce a customized MOF decorated with biochar to utilize the properties of both materials synergistically and implement in a leaching column experiment for immobilization of Cu in a real highly polluted technogenic soil to ultimately curtail Cu migration in the environment.

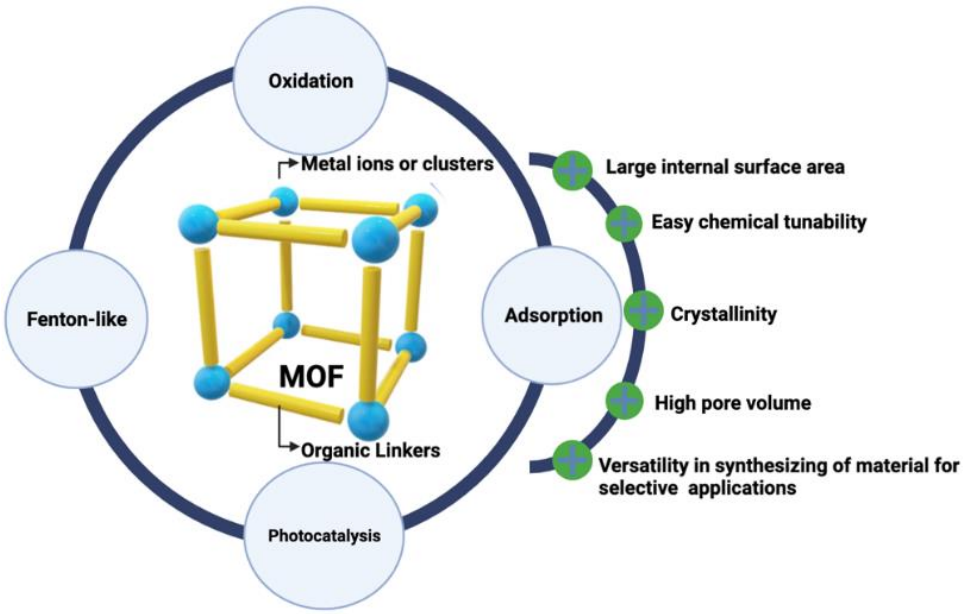

Figure 1.1. MOFs processes based on nanocomposites for remediation application (Bayero et al., 2021)

1.2. Research Questions

What effects do MOFs have for immobilization and fixation of heavy metal ions? Does biochar provide the synergistic effect in the nanocomposite for heavy metal uptaking? Will biochar act as a good candidate for increasing the stability of nanocomposites? Will nanocomposite show selectivity towards heavy metal ions? Can MOFs be stable in the soil and water medium?

1.3. Research Objectives

The objective of study is to investigate biochar-based nanocomposites and implement the best optimized composites in real heavy metal contaminated soil and water. This is carried out as follows: to synthesize and characterize the biochar-based MOFs nanocomposites according to previous studies with slight modification; to optimize the as-prepared materials based on different information gained from different characterization techniques such as XRD, FTIR, SEM, and TEM along with pre-testing during synthesis; to apply the as-prepared materials as a sorbent in heavy metal polluted aqueous solution; and to apply the best-optimized nanocomposite in the soil matrix during the soil leaching column experiment. Finally, handle all the info generated above to evaluate the performance of the best-optimized nanocomposite and unveil the chemistry involved in the immobilization of heavy metals in real

contaminated technigenic soils.

1.4. Novelty of the Thesis

The current study is designed to solve the problems associated with the elevated concentration of heavy metals in soil nd water samples. In order to address the problem, we will synthesize a set of biochar-based nanocomposites with high efficiency and selectivity towards heavy metal ions. The several key properties, including high specific surface area, excellent porous nature, have rendered biochar to present distinguished performance characteristics for acting as the basis for growing the nano-sized particles. The composite represents a unique and original project idea that, if successful, will offer a new application for biochar. The notion that biochar-MOF acts as amendments for the soil contaminated with heavy metals have never been proposed. The performance of all the sub-processes will be assessed in the one integrated approach; then, all materials will be applied to the soil leaching column experiments. In this context, simultaneous sorption of heavy metals into the composite will be demonstrated. The inherent interdisciplinary character of the thesis will touch at least five different fields, 1) chemistry, 2) material science/engineering, 3) physics, 4) analytical chemistry, and 5) soil science/engineering.

1.5. Methodological Approach of the Thesis

To ensure that the research and innovation aims of the project will be fulfilled, the work-plan is divided into four work packages (WP). WP1 will be focused on the synthesis and characterization of biochar-based MOFs nanocomposites according to previous studies with slight modification (Mahmoodi, Oveisi, Panahdar, Hayati, & Nasiri, 2020a; Mahmoodi, Taghizadeh, & Taghizadeh, 2019a). WP2 is focused on applying the as-prepared materials as a sorbent in heavy metal polluted aqueous solution (Li et al., 2021a; S. Zhang et al., 2021a). The information gained in WP1 and WP2 from different characterization techniques such as XRD, FTIR, SEM, and TEM along with the information related to the adsorption capacity of the materials will be used in WP3. WP3 will be devoted to applying the best-optimized nanocomposite in the soil matrix during the soil leaching column experiment (Ahmad et al., 2014; Anae et al., 2021a; Bashir, Hussain, Shaaban, & Hu, 2018; Beesley & Marmiroli, 2011; Bian et al., 2013; Merdy, Gharbi, & Lucas, 2009; Yutong et al., 2016). Subsequently, WP4 will handle all the info generated from WP1 to WP3 to evaluate the performance of the best-optimized nanocomposite and unveil the chemistry involved in the

immobilization of heavy metals. We propose the process in which the successful performance of the system totally depends on the synthesis of biochar-based composite. The former challenge represents a high-risk assumption since unsuccessful synthesis will lead to the functional deterioration of hybrid. The corresponding solution will be addressed by using other synthesis methods to form a better hybrid.

1.6. Scope and Limitations of the Thesis

The research will explore remediation of heavy metals contaminated water and soil by applying biochar-based nanocomposites. The remediation methods will only focus on the adsorption for the water and sorption for the soil. Moreover, the biochar will be composited with metal-organic frameworks (MOFs).

2. LITERATURE REVIEW

2.1. Biochar application in remediation of heavy metals-contaminated soils

This section was written based on our review article (Mazarji et al., 2021).

Biochar possess a variety of physico-chemical properties in accordance to the feedstock biomass and the chosen thermochemical pyrolysis conditions (Anae et al., 2021b). As a result, both the manufacturing (Yaashikaa, Kumar, Varjani, & Saravanan, 2020) and field applications of biochar have a significant impact on its performance, and the source material composition (Ho, Zhu, & Chang, 2017). To better comprehend the existing diversity of biochars and the corresponding impact for its use as an remediation material for amendment, the link between biochar properties, manufacturing conditions, and biomass feedstock composition and classification must be established (T. Xie, Reddy, Wang, Yargicoglu, & Spokas, 2015).

Chen et al. (2020) established that, higher levels of Cd(II) soils might likely increase the potential of the metal to transfer and bio-accumulate in plants systems, as well as its tendency to leach into surface water and groundwater, posing a threat to ecosystems (D. Chen et al., 2020). To remediate this risk, Chen et al. (2022) carried out a study to understand the relationship between biochar pyrolysis temperature and Cd(II) transport in water-saturated soil (M. Chen et al., 2022). They discovered that at high ionic strength, biochar produced at a temperature of 500°C significantly reduced Cd(II) migration within the soil matrix (M. Chen et al., 2022). Biochar of pine sawdust generated at 550°C outperformed biochar produced at 300°C for Pb immobilization. Notably, biochar produced at higher temperatures has the tendency to have a better stability, making it ideal for rehabilitating soils contaminated with Pb that are frequently flooded (Beiyuan et al., 2020). Heavy metals, such as As, presents a high risk to human and animal health when discharged into the environment. The sorption affinities of biochar generated from corn straw were found to be satisfactory for As(III). Furthermore, a pH increase following biochar application can counteract acid soil, which potentially reduces the acidification of red soil (Yu, Zhou, Huang, Song, & Qiu, 2015). We have elabotad the potential of biochar as a sustainable amendment to soils contaminated with heavy metals in our recent review (Mazarji et al., 2021).

2.2. Biochar Nanocomposites application in remediation of heavy metals-contaminated soils

This section was written based on our review article (Mazarji et al., 2021).

In our recent review Mazarji et al. (2021) we further elaborated on biochar nanocomposites (Mazarji et al., 2021). We discussed the role of nanocomposites on enhancing the capacity of biochar and both biochar and nanocomposites having a synergistic effect on the immobilization of heavy metals in soil systems. Biochars were made from kenaf bar, green tea, residual bark, cornstalk, wheat straw, sawdust, palm fiber, etc with pyrolysis temperatures ranging from 400 to 800 °C, according to the findings in our review. Nano-metal oxides/hydroxides, functional nanoparticles, and carbon nanomaterials are the three types of nanomaterials that have been identified. Co-precipitation, one-step pyrolysis, and liquid-phase reduction procedures are among the methods used in the synthesis. Figure 2.1. illustrates the conversion of agricultural waster biomass into biochar and subsequently compositing with nanocomposites.

Arabyarmohammadi et al. (2018a) improved Pb immobilization in mine-affected soils by using chitosan, nanoclay, and biochar to make a composite. After 24 hours of leaching, the efficiency of 52.29 to 98%, outperformed the biochar efficiency 30 to 41.16% (Arabyarmohammadi et al., 2018). Qian et al. (2022) fabricated a biochar nanocomposite (BC-nZVI) to immobilize Cd and Pb in farmland and real contaminated soil (Qian, Liang, Zhang, Huang, & Diao, 2022b). Treatments with BC, BC-nZVI in artificially spiked soil, and BC-nZVI in actual contaminated soil reduced Cd mobility in the soil by 34, 86.49 and 100%, respectively. This is linked to the pH increase caused by biochar-based material, which facilitated in the production of Cd precipitates (Qian et al., 2022b). Furthermore, after treatment with BC-nZVI, the exchangeable fraction (EX) of Cd reduced to 10.25 % from 59.14 %, according to the sequential extraction process used (Qian et al., 2022b). After incorporating graphene oxide to produce a composite for Cu immobilization in soil, Mandal et al. (2020a) pyrolyzed cornstalk at 450°C and then loaded nZVI onto the biochar (Mandal, Pu, He, Ma, & Hou, 2020a). After 14 days of incubation, the soil test revealed that the immobilization of the produced composite and biochar alone was 75.16% and 55.15%, respectively. The findings revealed that the acidic and oxygen-based functional groups found on the biochar surface provided an effective pH that allowed other ions present, such as Ca^{2+}, NH_3, H_2, CO, and CO_2 to better immobilize. (Mandal, Pu, He, Ma, &

Hou, 2020b). Lu et al. (2018) explored on whether pyrolysis temperature, feedstock selection, or magnetization had an impact on sorptive biochar capacity. For limiting Cd, Pb, and Zn leaching, magnetization was less significant than identifying the appropriate pyrolysis and feedstock temperature. (Lu et al., 2018). According to Fan et al. (2020) while biochar has proven to be effective for heavy metal cleanup, it has been less effective for As immobilization in the vast majority of instances (Fan et al., 2020b). In this regard, compositing biochar with nanocomposite showed a promising result in eliminating As from heavy metal contaminated soil (Fan et al., 2020b).

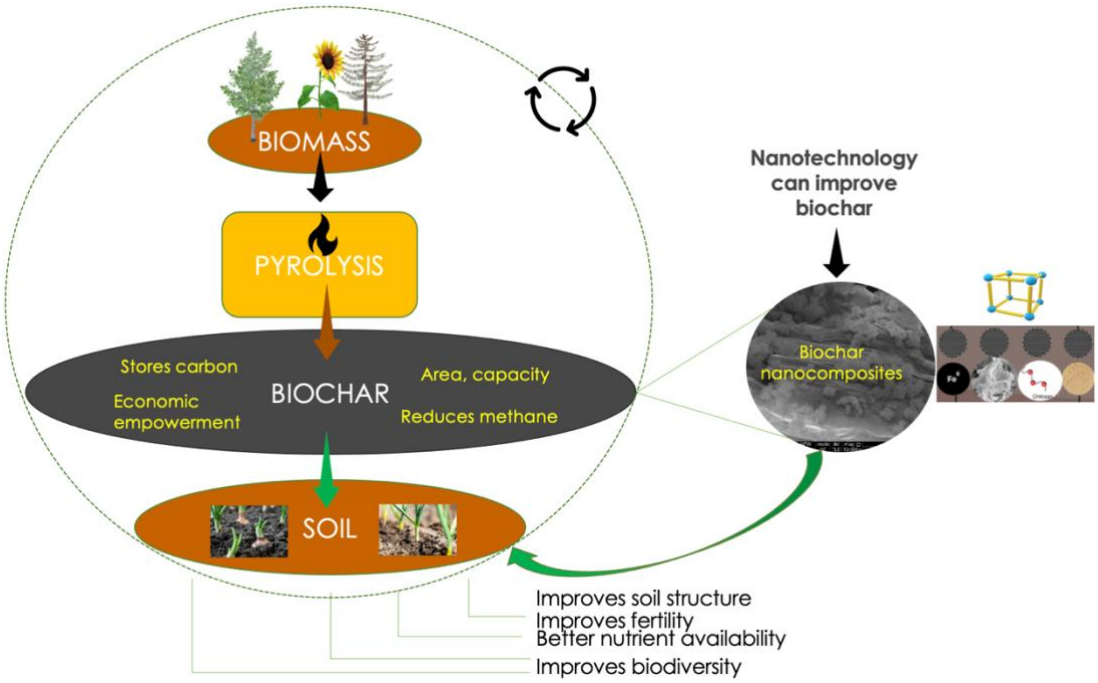

Figure 0.1. Agricultural waste biomass as a source of biochar and bio-based nanocomposites.

2.3. Biochar and Metal-organic Frameworks

This section was written based on our review article (Mazarji et al., 2021) and conference paper (Bayero et al., 2021), respectively.

When compared to pristine MOFs, MOF-based composites have demonstrated a significant enhancement in capacity to eliminate heavy metals from environmental matrices. For example, in advanced oxidation processes, a composition of MOF and other nano-enabled material such as graphene oxide (GO) will enable the aromatic sp2

domains, and ionic groups to react via bonding contacts, acting as nodes to link with the organic groups present on MOFs and enhance the reaction rate (D. Huang et al., 2021). In this context, we carried out a review on the recent studies that utilized MOFs for remediation of media contaminated with heavy metals (Bayero et al., 2021). Briefly, Moradi et al. (2016) used a water-stable MOF-235(Fe) which is sulfonated and then loaded on Fe_3O_4 to create a magnetic nano sorbent. Cd^{2+} could easily be removed from water medium using the extraction methods that adopts magnetic solid-phase (Moradi, Shabani, Dadfarnia, & Emami, 2016). Despite very high concentrations of Na^{+}, a water-stable MOF, MIL-100(Fe) which is functionalized, and then complexed together with polydopamine (PDA) to produce a Fe-BTC(MIL-100(Fe))/PDA (composite), demonstrated not only quick , and selective affinity towards of Pb^{2+} and Hg^{2+} but also eliminated the influence of potential metal ions that might be in competition Pb^{2+} and Hg^{2+} (Sun et al., 2018). Wei et al. (2019) Carried out a study on Cu^{2+} adsorption using amine functionalized GO, ZIF-8, and 3-aminopropyl-triethoxysilane. The composite (ZIF-8@GO) demonstrated remarkable Cu^{2+} removal efficiency of around 1872.24 mg/g) which also demonstrated high reusability (Wei et al., 2019).

As demonstrated in Figure 2.2., the composition of MOFs with various materials gives diverse chances to address many of the problems associated with pure MOFs. Redox-related tendencies are high in iron-based metal-organic frameworks (Fe-MOFs) (C. Zhang et al., 2019). The Fe^{2+} and Fe^{3+} forms, on the other hand, are easily accessible and exploitable in MOF structures. This benefit, combined with their low toxicity, results in better structural stability and environmental friendliness than other MOFs for remediation. Based on biochar's capacity as a widely used soil amendment, the biochar-MOF bio-based composite would provide the following benefits: 1) Because of the potential synergistic effect of Fe-MOFs and biochar, high capacity for immobilization is expected; 2) Preventing Fe-MOFs from aggregating in the soil system; 3) The long-term stability of the resulting composite is likely be improved; and, 4) Enhancing the selectivity towards heavy metal ions.

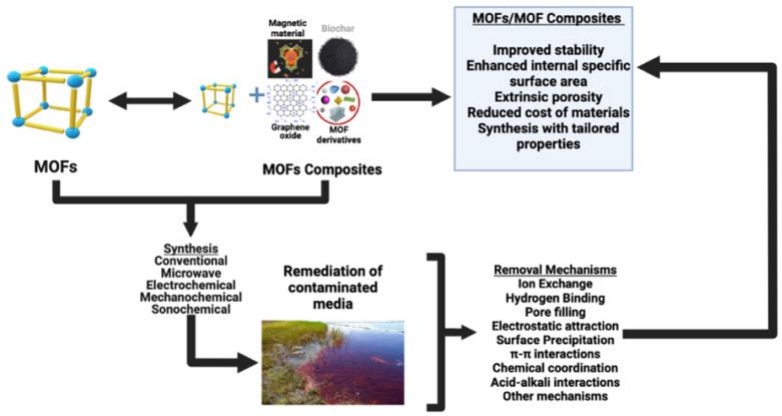

Figure 2.2. Future prospects for implementation of MOF and biochar bio-based composites for remediation of soils contaminated with heavy metals (Bayero et al., 2021).

3. MATERIALS AND METHODS

3.1. Site Description and Soil Classification

The soil samples were collected from a location with the coordinates 48°20'42.15" N, 40°14'14.46" E, which is a dry Atamanskoe lake in Kamensk-Shakhtinskii, Rostov area, southern Russia. Figure.3.1. This lake was once a waste reservoir that collected effluents from industrial plants manufacturing semi-synthetic and synthetic textiles for four decades.(Linnik, Saveliev, Bauer, Minkina, & Mandzhieva, 2021). In the mid-1990s, the industrial activity near the waste reservoir ended, and the reservoir dried up since there was no more inflow of effluent (T. Minkina et al., 2019). The soil is classified as Spolic Technosol based the world reference base of soil resources (2014 updated 2015) (FAO, 2015). The prefix Spolic, is the principal qualifier which is an indicator of how the soil named as a Technosol. The prefix sp represents a soil layer 20 cm thick or greater, within the region of 100 cm or less of the surface of the soil, comprising 20% or greater (by volume, as well as weighted average) of artefacts including 35% or greater (by volume) of industrial waste, such as mining spoil heaps, dredgings, and so on (IUSS, 2014).

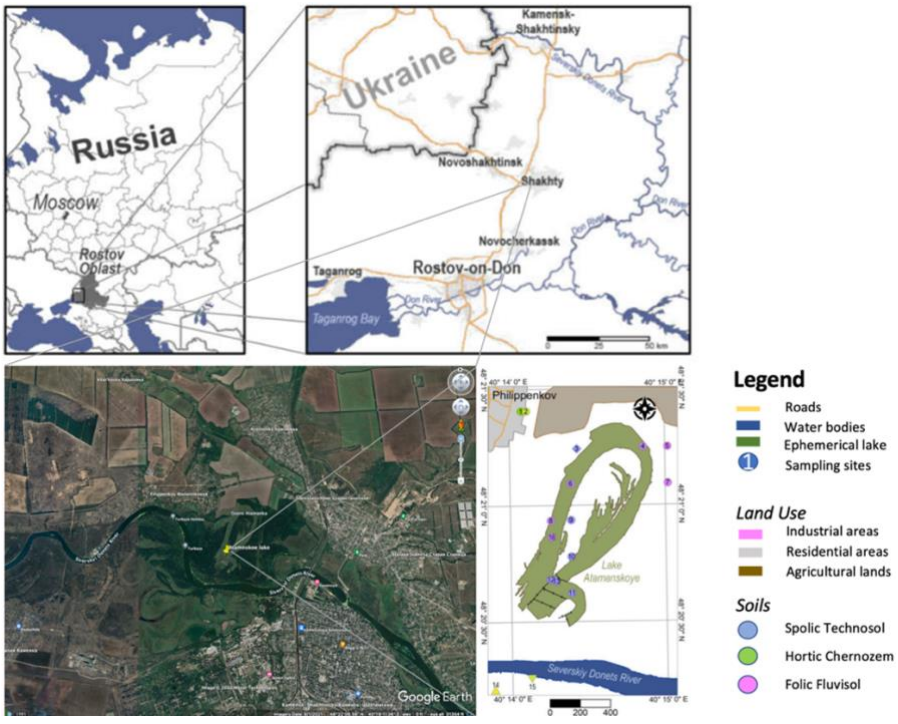

Figure 3.1. The lake Atamanskoe, surrounding environment and the monitoring sites depicted by circles.

3.2. Soil Sampling Procedure

Soil samples were obtained from the upper layer of the soil (0–20 cm) on designated test plots of 50 cm by 50 cm. Using the envelope method, soil samples were collected by soil auger from the surface layer up to a depth of 20 cm (GOST 17.4.4.02–84, 2008). The five samples resulting from envelop method were mixed to form a homogenous mixture. After the completion of sampling, all samples collected were immediately moved to the laboratory. The samples were air-dried in the laboratory, and any contaminants such as small branches, plants, and root remains were physically removed before being passed via a 1 mm sieve. Finally, to preserve the soil's naturalness, it was kept at a steady temperature (4 °C) before the commencement of analysis.

3.3. Soil Sample Characterization

The soil characterization results of the sampled soils are presented in Table 3.1.

Table 3.1. Soil sample characterization

Soil properties	Amounts and units
Age	40 years covering the period from the beginning to the end of polluting activity
pH	6.55 (Soil:Water = 1:5)
Sand fraction (1.00 – 0.05 mm)	73.6 %
Fraction of silt (0.05 – 0.002 mm)	18.8 %
Fraction of clay (<0.002 mm)	7.6 %
Total organic carbon (TOC)	3.5 %
Cation exchange capacity (CEC)	18.8 mmol(+)kg^{-1} (Ca^{2+}), and 2 mmol(+) kg^{-1} for Mg^{2+}
SiO_2	62.03 %
TiO_2	1.21 %
Total Cu concentration	286 $mgkg^{-1}$

3.4. Preparation of Biochar-based Metal-organic Framework Composites

The biochar preparation was carried out in accordance with the method described by Mazarji et al. (2022) (Mazarji et al., 2022). Briefly, an artisanal pyrolyzer vessel was loaded with rice husks. The materials were slowly pyrolyzed at 15°C min^{-1} and afterwards maintained at 700°C for 1 hour in an oxygen-limited atmosphere. After the vessel had cooled to 25°C, the pyrolyzed biochar was recovered. The resulting biochar by rice husks was denoted as RBC and used as such in the subsequent sections. It is worth mentioned that the RBC was used as received for the preparation of the biochar-based metal-organic framework composites only. Hence, no further individual analysis (such as characterization, amendment) was carried out using RBC alone within the scope of this study.

The synthesis of the biochar-based metal-organic framework composites was prepared in accordance with the synthesis method by Mahmoodi et al. (2020) with minor modification (Mahmoodi et al., 2020b). Briefly, 0.05 g of RBC was allowed to soak overnight in 30 mL of N,N-dimethylformamide (DMF, about 99.8%, Sigma-Aldrich). After the completion of soaking, 0.412 g (2.48 mmol) of 1,4-benzene dicarboxylic acid/ terapthalic acid (H_2BDC, Sigma-Aldrich) was added into the solution, followed by 1.3 g (4.9 mmol) iron (III) chloride hexahydrate ($FeCl_3.6H_2O$, Sigma-Aldrich) The solution obtained from the above mixture was tranferred into an autoclave and placed into an ultrasonic bath for a total period 2 h (4 times of 30 mins each with 5 mins rest). The resulting solution was transferred into a vacuum oven, for 20 hours at 110 °C throughout. After left to be cooled naturally at room temperature, the obtained brownish solid products were washed and centrifuged multiple times with DMF. After the completion of washing, the products were dried at 120 °C for 24 hours in a vacuum oven. The resulting product was denoted as RBC-MIL. Sunsequently, without the addition of biochar, the pristine MIL-101(Fe) was synthesized following the above steps accordingly and the resulting product was denoted as MIL.

3.5. Characterization of MIL and RBC-MIL

To explore the crystallite phase of materials, a Brucker D2 Phaser diffractometer was used to take X-ray diffraction (XRD) measurements in the range of 20° to 90° with a 0.01° step. To evaluate the existence of functional groups, Fourier transform infrared spectroscopy (FTIR) was obtained in the interval of 4000 to 500 cm^{-1} with a constant resolution of 4 cm^{-1} using a VERTEX 70v Bruker's spectrometer. The surface

morphology of materials was studied in depth by a scanning electron microscope (SEM) by Carl Zeiss EVO-40 XVP and Nova Nanolab 600 FEI Netherlands). The Transmission electron microscopy (TEM) was used to visualize the samples using a Tecnai G2 microscope (Phillips, Netherlands) to observe the products' unique morphologies.

3.6. Experimental Design

To create the experiment model, the response surface methodology (RSM) was adopted in this study. The central composite design (CCD) was selected to fit a quadratic orientation and determine the interaction effects of the two independent variables chosen fort his study. The sorbent-to-soil mass ratio (x_1) and leaching time (x_2) were chosen as independent variables. The ranges and values of independent variables are shown in Table 3.2.

Table 3.2. Experimental ranges and corresponding levels of the independent variables

Independent variables	Factors	Unit	Ranges and levels				
			−α	−1	0	+1	+α
sorbent to soil mass ratio	x_1	%	0.59	1	2	3	3.1
Leaching time	x_2	days	0.96	2	4.5	7	8.04

$\alpha = 1.41$

For the ease of statistical computations and further model development, the real or actual values of the chosen independent variables (Xi) were coded into dimensionless unit of values (xi) within the range of +1 and 1 using Eq. (1):

$$x_i = \frac{X_i - X_0}{\delta X} \quad \textbf{(3.1)}$$

where X_0 and δX stands for the actual value of Xi corresponding to the center point and then the step change, in that order (Hanrahan & Lu, 2006a).

The formula 2k + 2k + n was used to design the experiments, with k and n denoting the number of the chosen independent variables along with the center runs (k = 2 and n = 5), respectively. In total, 13 experiments were carried out, which can be listed as four factorial points (2k), followed by four axial points (2k), and then finally five replications of the center point. The calculated value of α was found out using the

Eq (2) (Hanrahan & Lu, 2006b).

$$\alpha = 2^{\frac{k}{4}} \tag{3.2}$$

This implied, α equals $(2)^{2/4}$ = 1.41. The mathematical relationship that exists between the two chosen independent variables (x_1 and x_2) and the Eluate concentration (Y) is represented using Eq. (3) as:

$$Y = \beta_0 + \sum_{i=1}^{n} \beta_i x_i + \sum_{i=1}^{n} \beta_{ii} {x_i}^2 + \sum_{i=1}^{n} \sum_{j=i+1}^{n} \beta_{ij} x_i x_j \tag{3.3}$$

The meaning of xi and xj stands for the coded chosen independent variables ith and jth, respectively. β0, βi, βii, and βij corresponds to the intercept in the first term, the first-order model coefficient in the second term, the quadratic coefficient of variable i in the third term, and the interaction coefficient of variables i and j in the forth term, in that order (Hanrahan & Lu, 2006b; Jones, 2002). The reliability of the fit of the model was determined using the ANOVA and R^2 (the coefficient of determination. All the simulated experimental runs are presented in Table 3.3. The Design-Expert 7 (Stat-Ease, Inc.) software tool was used to evaluate the experimental data.

Table 3.3. Response surface methodology design matrix and corresponding experimental results.

CRun#	Coded values		Real values		Cu, experimental	Cu, predicted
	x_1	x_2	Sorbent to soil mass ratio (%)	Leaching time (days)	Soil + RBC-MIL	Soil + RBC-MIL
1	0	0	2	4.5	0.85 ± 0.01	0.83
2	0	0	2	4.5	0.82 ± 0.02	0.83
3	0	1.41	2	8.04	0.15 ± 0.02	0.17

4	-1	1	1	7	0.5 ± 0.03	0.48
5	0	0	2	4.5	0.83 ± 0.02	0.83
6	-1.41	0	0.59	4.5	1.70 ± 0.04	1.71
7	0	0	2	4.5	0.81 ± 0.04	0.83
8	0	0	2	4.5	0.82 ± 0.05	0.83
9	-1	-1	1	2	2.20 ± 0.04	2.20
10	0	-1.41	2	0.96	1.21 ± 0.02	1.19
11	1.41	0	3.41	4.5	0.32 ± 0.06	0.30
12	1	1	3	7	0.51 ± 0.03	0.49
13	1	-1	3	2	0.21 ± 0.02	0.21

3.7. Fixed Bed Leaching Column Studies

The efficiency and stability of as-prepared materials for retention of Cu during a continuous flow of effluent in consecutive leachate samples were evaluated using fixed bed leaching columns for retention of Cu during a continuous flow of effluent in successive leachate samples. This study investigated leaching behavior in fixed-bed columns using a 20 mm glass column with a 400 mm height as shown in Figure 3.2. The bed was filled with a uniform mixture of 5 mm glass spheres and a variable sorbent-to-soil ratio mixture. The ends of the column were secured using glass wool (Sigma-Aldrich). To keep the leaching solution from crushing the column surface, the soils were placed in the columns and then sealed with filter paper. Before leachate sampling, the soils were totally saturated.

The leaching experiment began with varied percentages of as-synthesised materials being added to the soil in accordance to the 13 treatments created in the design matrix presented in Table 3.3. The samples were incubated for 10 days after thoroughly mixing the soil with the required amount of RBC-MIL. As a control, one soil sample was left untreated with sorbents. Two treatments were produced for the dynamic leaching column experiemnts in this regard: control soil, and control soil + RBC-MIL. Throughout the testing, the amount of contaminated soil without any spike was kept constant at 25 g, which corresponded to a height of 10 cm, based on the anthropogenic occurrence of contaminations. After ten days of incubation, the

materials were fully dried and prepared for implementaion in the fixed bed column tests.

The pH of the leaching water was chosen to be 5.5 to mimic natural precipitation as much as practicable. De-ionized water with a pH of 5.5 was continuously pumped downwards from the top of the columns using a peristaltic pump. Eluate samples (15 mL) from soil were collected after passing through the columns for 14 consecutive days. The drains were collected and the filtered with a Whatman® Grade 42 filter on a daily basis prior to measurement. A Kvant-2m1 spectrometer was used to make this measurement, which uses a flame atomic absorption spectrometry technique (Cortec, Russia).

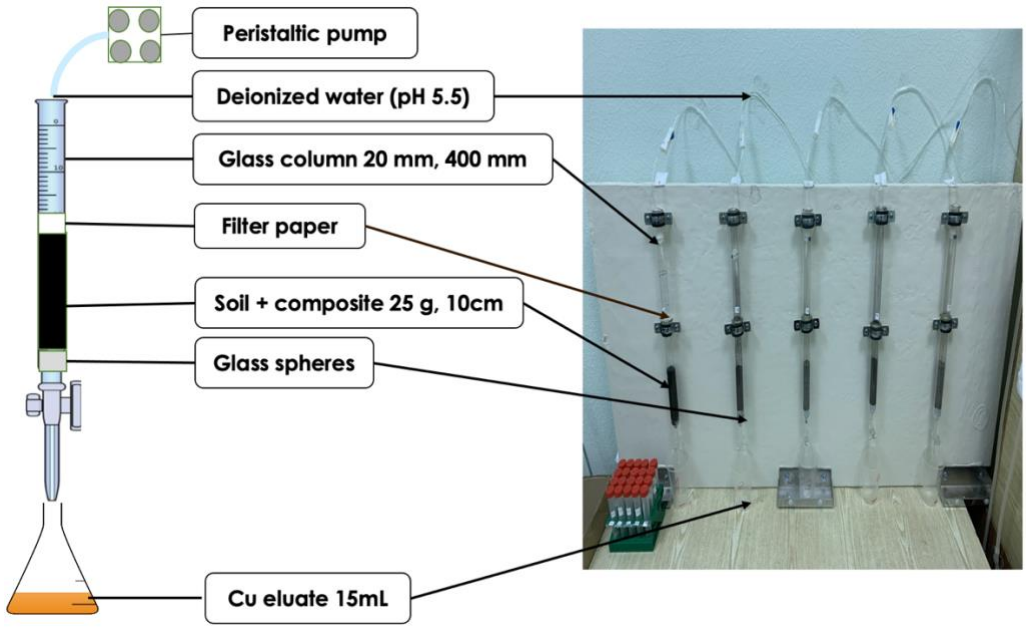

Figure 3.2. A schematic illustration and the real fixed bed column used in this study.

3.8. Fractionation studies

Following the completion of the leaching experiment, the soil sample was treated sequentially to determine the fractions bound with exchangeable ions, adsorbed ions, carbonates, Fe/Mn-(hydr)oxides and organic matter using Tessier's method as shown In Table 3.4. The five Tesier fractions were grouped into acid soluble (F1 and F2), reducible (F3), oxidable (F4) and residual (F5) (Tessier, Campbell, & Bisson, 1979).

Table 3.4. Tessier et al. Sequential extraction method

Fraction	Extraction method	Extracted component
F1, Exchangeable	1 M $MgCl_2$, pH 7, 1 hour	Exchangeable ions
F2, Adsorbed/Carbonatic	1 M NaOAc, pH 5 (HOAc), 5 hours	Adsorbed ions, carbonates
F3, Reducible	0.04 M NH_2OHHCl in 25% (v/v) HOAc, 6h, 96°C	Iron-manganese oxides
F4, Sulfidic/organic	30% H_2O_2, pH 2 (HNO_3), 5 hours at 85°C, extracted with 3.2 M NH_4OAc in 20% HNO_3 (v/v), 0.5 hours	Sulfides/organics
F5, Residual	Hot HF-$HClO_4$ con.	Metals bound in lithogenic minerals

3.9. Analytical Methods

An X-ray fluorescence (XRF) scanning spectrometer, the Spectroscan MAKC-GVM, (Llc Spectron, Russia) was employed to measure the total Cu concentration of the polluted soil without any spike to achieve realistic soil conditions of the studied area. The methods proposed by Black et al. (1965) were used to calculate the available clay and CEC (Black, Evans, & Dinauer, 1965) and ISO 23470 (ISO 23470, 2018), in that order. The pH (pH in H_2O) determination of the soil was carried out using a ratio 1:5 suspension of soil in water following the standard of (ISO 10390, 2005). The fixed pipette approach was used to estimate the size distribution of soil particles in accordance with the standard ISO 13317-2 (2001). Total organic carbon (TOC) was determined by the use of a total organic carbon analyzer TOC-L CPN Shimadzu utilizing a high-temperature catalytic burning approach. The difference between total carbon and inorganic carbon was used to calculate the TOC.

3.10. Statistical Analysis

All data were processed using OriginPro (OriginLab Corporation, USA) or Microsoft Excel (Microsoft 365, © Microsoft 2022). The results are given using one-way ANOVA on the mean and standard error (S.E.). The Tukey's HSD test was utiliozed to compare means, and differences of the dataset and $p < 0.05$ values were considered to be significant.

4. RESULTS AND DISCUSSION

4.1. Preliminary Screening for the Best Optimized Synthesis Procedure

The approach (RSM) we adopted for this study totally depended on the successful workability of the synthesis conditions (RBC dosage, time, temperature, and the bearing pressure of the autoclave) and performance of the produced RBC-MIL composite. The failure in the synthesis procedure represented a high-risk assumption since unsuccessful synthesis always led to the functional deterioration of the hybrid. In this context, we carried out different scenarios of synthesis by varying the RBC dosage. The ratio of $FeCl_3.6H_2O$ to H_2BDC (organic linker) were kept constant at 4.9 mmol to 2.48 mmol throughout the synthesis procedure. The RBC dosages considered were 0.4, 0.3, 0.2, 0.15, 0.1, and 0.05 g corresponding to A-1, A-2, A-3, A-4, A-5, and A-6 respectively in Figure 4.1. As shown in Fig. 3.1, A-1 (0.4 g biochar, 20 hours, 110 °C, and 30 mL DMF) exhibited a poor performance for Cu removal. This condition was attributable to the excessive dosage of RBC in the synthesis solution. Hence, the expected structure of RBC-MIL composite could not form.

The same trend was observed for A-2, and A-3 but remarkably improved for A-4, and A-5 as the RBC dosage dropped in the synthesis solution. After several trials of different RBC dosages as well as the varying conditions mentioned above, A-6 (0.05 g biochar, 20 hours, 110 °C, and 30 mL DMF) performed the best. It is worth noted that, addition of more than 0.05 g of RBC into the synthesis solution resulted in the formation of a dispersed blackish solid phase or aqueous brownish surface in the final product after activation. The appearance of these conditions was supposed to be the unreacted RBC or $FeCl_3.6H_2O$ during the synthesis. Hence, 0.05 g was chosen as the optimum threshold for the content of RBC in the synthesis solution. This result suggested that RBC-MIL composite was best produced with less amount of RBC to guarantee a functioning hybrid and acted as the host for the growth of MIL-101(Fe) crystals without interfering with their formation and development.

Due to the better removal efficiency evidenced for different synthesis of RBC-MIL composites, the subsequent experiments were carried out by using the RBC-MIL optimized under A-6 conditions. Although biochar was composited with MOF for the first time, these results of the synthesis were consistent with other synthesis results of some similar reports such as (Mahmoodi et al., 2020b; Mahmoodi, Taghizadeh, & Taghizadeh, 2019b).

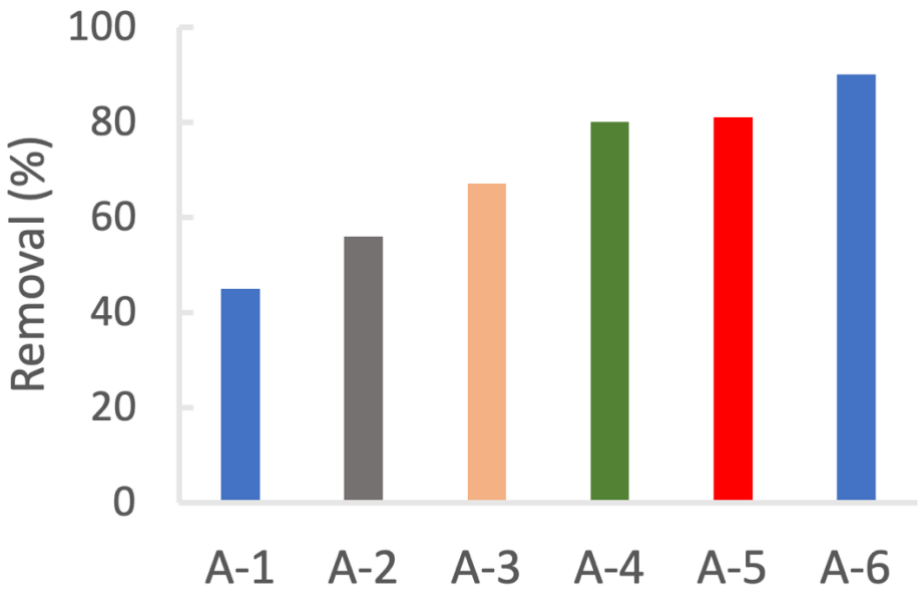

Figure 4.1. Cu removal for different synthesis of RBC-MIL composites (C_i = 10 mg L^{-1} Cu, time = 20 hours, RBC dosage = 0.05 g L^{-1}).

4.2. Characterization

The crystalline phases of the materials were identified using XRD analysis. Figure 4.2. shows the XRD diffraction spectrum of MIL, which demonstrated prominent peaks at 5.0°, 8.9°, 9.5°, 10.6°, and 16.3°.The MIL's XRD pattern is in aggreement with the synthesized Fe-based MIL101 materials reported in literature such as the works by (Mahmoodi et al., 2020b; Q. Xie et al., 2017; C. Zhang et al., 2019). Similarly, as illustrated in Figure 4.2., the RBC-MIL the pattern of XRD confirmed the presence of MIL's peaks, albeit at a lower intensity. There were no additional diffraction peaks for RBC-MIL, demonstrating that joining RBC to MIL had no effect on MIL's structure. The formation of a zeotype octahedral structure of MIL-101(Fe) on the surface of RBC and MIL-101(Fe) alone was confirmed by XRD patterns of composites.

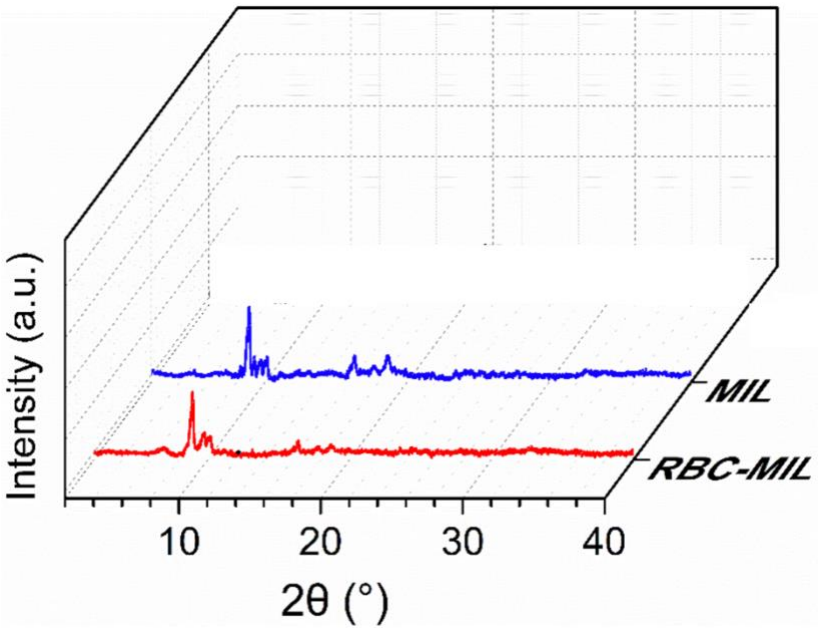

Figure 4.2. XRD spectra of MIL, and RBC-MIL composite.

The functional groups in the materials were identified using FTIR spectroscopy. The FTIR spectra of MIL and the RBC-MIL composite are shown in Figure 4.3. Based on the obtained FTIR result, MIL revealed characteristic carboxylate group vibration bands at 1300–1700 cm^{-1} and benzene ring vibration bands at 770 cm^{-1}. The peak that is at approximately 1657 cm^{-1} depicted the C=O bonds. According to Wang et al. (2018) the peak at 1100 cm^{-1} was related to the C–H in-plane bonding mode in the case of MIL (Wang et al., 2018). According to a comparable investigation by Mahmoodi et al. (2019), the strong peaks at 1650–1500 cm^{-1} in MIL and RBC-MIL composite were linked to the vibration of the C=C aromatic ring (Mahmoodi et al., 2019b). The peaks at about 750 cm^{-1} is linked with C–O–C vibration. The peaks ranging from 1200 to about 1000 cm^{-1} are mostly in relation with the C–O stretching vibration of ether groups in both MIL and RBC-MIL (Saedi, Tangestaninejad, Moghadam, Mirkhani, & Mohammadpoor-Baltork, 2012). The availability of several functional groups (C–O–C, OH, C=C, C-H, and C–O) afforded the RBC-MIL a negative surface charge, resulting in a better potential for Cu immobilization.

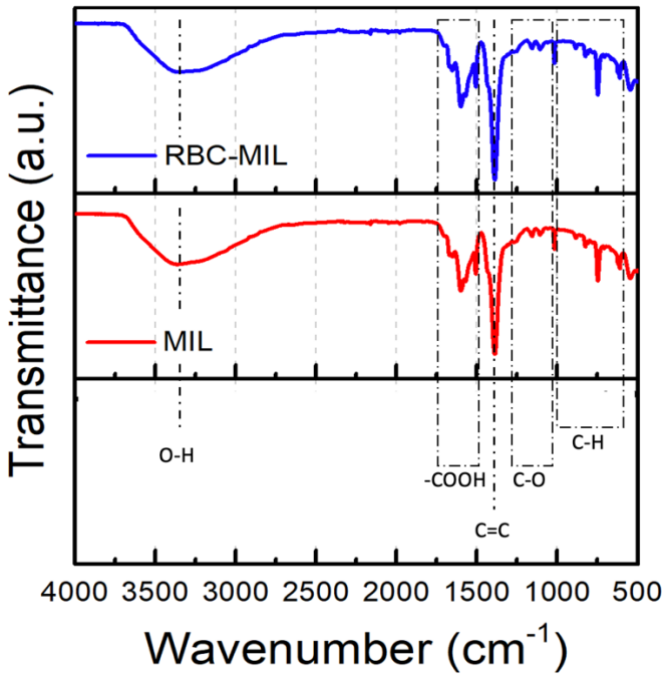

Figure 4.3. FTIR spectra of MIL, and RBC-MIL composite.

The SEM images were taken to explore the morphology of the materials.SEM images of MIL revealed an unique octahedral crystal structure, as depicted in Figure 4.4.a Figure 4.4.a along with Figure 4.4.b shows the SEM images of MIL, and RBC-MIL composite, respectively. SEM images of MIL revealed an unique zeotype octahedral crystal structure, as shown in Figure 4.4.a The composite materials, on the other hand, had the same shape as MIL crystals on the biochar substrate (Figure 4.4.b). MIL had a greater homogeneous octahedral crystal size, as illustrated clarely in Figure 4.4.b, due to the surface of the derived carbon-based material functioning as a nucleation agent (Muñoz-Senmache et al., 2020; Pachfule, Balan, Kurungot, & Banerjee, 2012). The particle size of the MIL 101(Fe) crystals reduced, while the octahedral faces of MIL got more defined, as evidenced in SEM images of pure MIL and the composite form (RBC-MIL). The rapid nucleation and stability of MIL 101 (Fe) crystals on the biochar surface may be explained by the negative surface of biochar's great capacity to support metal cations (Mahmoodi et al., 2019b).

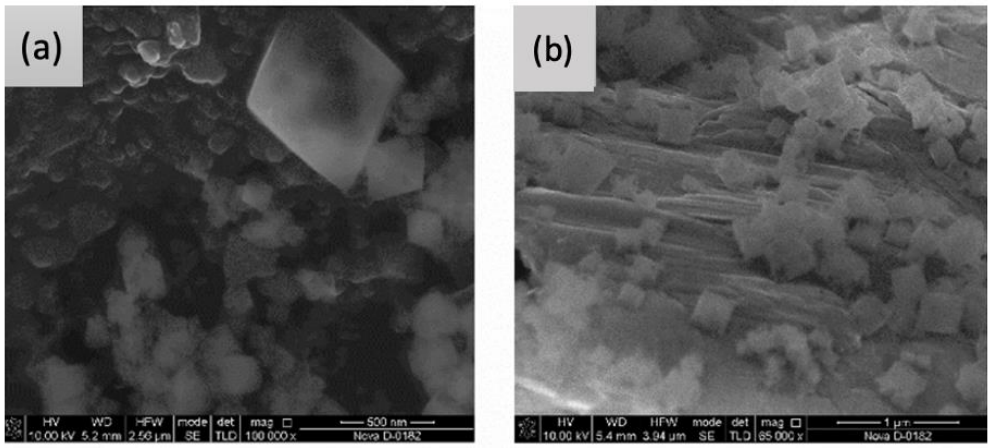

Figure 4.4. SEM images of MIL (a), and RBC-MIL (b)

The products' unique morphologies were investigated using TEM. MIL and RBC-MIL composite TEM images are shown clearly in Figure 4.5.a and Figure 4.5.b, in that order. As can be observed in the SEM images, the MIL particles in the TEM images were aslo structured like octahedrons and had a consistent mean size of 200 ± 15 nm. MIL particles were effectively distributed on the RBC surface and used as a core for biochar-MOF composite development. Noticeably, the particles clearly indicated that they were monodispersed and had the same morphology as MIL-101(Fe) with a zeotype octahedron shape. The nano-sized particles were reportedly deposited through the surface of biochar and exhibited an octahedral form that matched the SEM images.

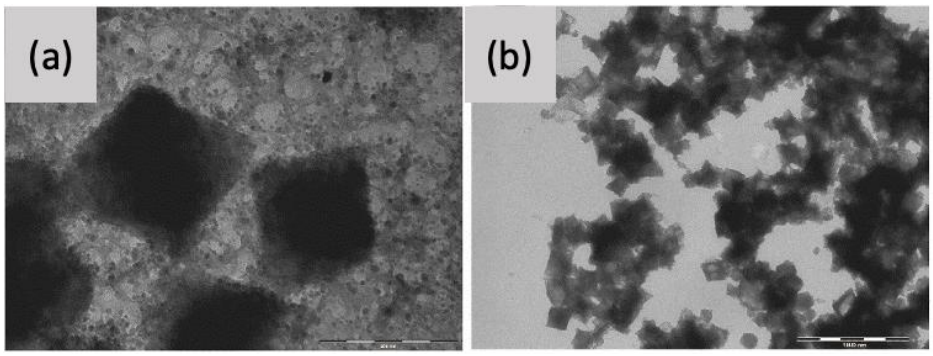

Figure 4.5. TEM images of MIL (a), and RBC-MIL (b) composite.

4.3. Model Development and ANOVA

The 13 CCD experimental scenarios are shown in Table 3.3. As explained in section 3.7, soil height, soil type, and flow rate were kept constant for the 13 experimental runs. The CCD had two independent variables including sorbent-to-soil mass ratio (x_1) and leaching time (x_2). The eluate Cu concentration (Y) which was the

response was used to construct the surface plots in the presence of RBC-MIL. The input data was placed into Table 3.3 when the experimental runs were completed, and quadratic modeling was performed. In order to link Cu leaching (Y) with the independent variables, the following regression equations, as shown in Table 4.1, were established at the end of the modeling.

Table 4.1. Real and coded regression models for the eluate Cu concentration in the presence of RBC-MIL composite.

Treatment variants	**Regression equations**	
Soil + RBC-MIL	*Coded factors*	
	$Y_1 = 0.83 - 0.50 \times x_1 - 0.36 \times x_2 + 0.5 \times x_1 x_2 + 0.09 \times x_1^2 - 0.07 \times x_2^2$	(Eq. 4)
	Real factors	
	$Y_1 = 4.40 - 1.76 \times A - 0.44 \times B + 0.2 \times AB + 0.09 \times A^{\,2} - 0.01 \times B^2$	(Eq. 5)

Y_1 = Elute Cu concentration in the presence of RBC-MIL (mg L^{-1})

x_1 = Coded sorbent-to-soil mass ratio

x_2 = Coded leaching time

A = Sorbent-to-soil mass ratio (%)

B = Leaching time (days)

To test the level of significance of the chosen independent variables and their experimented interactions, we used ANOVA to ensure that the models were valid. The results of the model adequacy validation of the ANOVA are represented in Table 4.2. Model terms were statistically significant as p-value < 0.0001, for the soil + RBC-MIL. The F-value of the model was 2644.81, for soil + RBC-MIL, which indicated the significance of the model. The observed high F-value was 0.01% likely attributed to noise for the model. As given in Table 4.2, all model terms showed p-values < 0.05, which indicated that all terms including x_1, x_2, x_1x_2, x_1^2, x_2^2 were significant. Moreover, the F-value of 1.83 for the lack of fit in the soil + RBC-MIL model, indicated that it is not significant in comparison to the pure error. The model had a 28.14% chance of having a substantial lack of fit F-value due to noise. As a result, the

lack of fit values were non-significant, indicating that the model fitted well.

Table 4.2. The ANOVA and quadratic models results

Treatment variants	Sources	Analysis of variance (ANOVA)				
		Sum of squares	**Degree of freedom**	**Mean squares**	***F*-value**	***p*-value**
Soil + RBC-MIL	Model	4.13	5	0.8254	2644.81	< 0.0001
	x_1	1.98	1	1.98	6344.48	< 0.0001
	x_2	1.04	1	1.04	3333.65	< 0.0001
	$x_1 x_2$	1.00	1	1.00	3204.36	< 0.0001
	x_1^2	0.0565	1	0.0565	181.06	< 0.0001
	x_2^2	0.0364	1	0.0364	116.76	< 0.0001
	Pure error	0.0009	4	0.0002		
	Lack of fit	0.0013	3	0.0004	1.83	0.2814
	Corrected total	4.13	12			
	Adjusted R^2	0.99				
	Predicted R^2	0.99				

Table 3.3 shows the experimental and projected values into the developed quadratic models for predicting the leachate Cu concentration in the eluate samples for the RBC-MIL model. As can be seen, the predicted and the experimentally obtained values were in very close agreement. The adjusted R^2 agreed with the predicted R^2, validating the models' correctness as plotted in Figure 4.6. R^2 revealed that the estimated regression equation exhibited a very good fit of the quadratic model as the regression line represent showed that R^2 was 0.99.

As a result, the model described here can be used to predict Cu concentration leaching. Overall, the analysis of variance results suggested that quadratic models are

suitable for creating three-dimensional response surface model graphs.

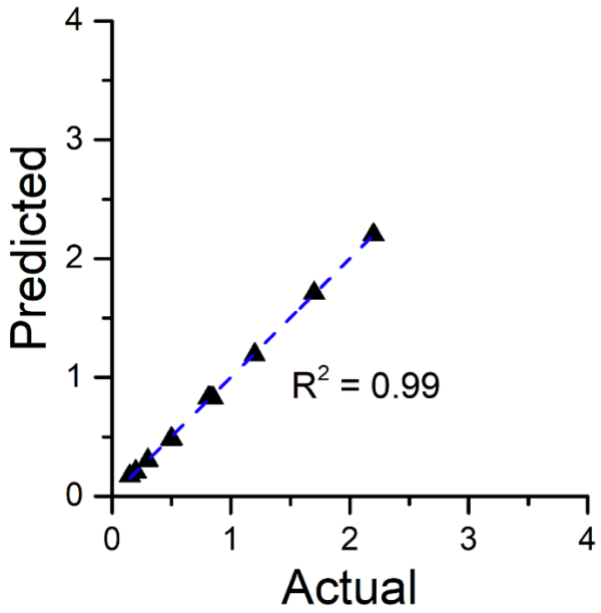

Figure 4.6. Experimental (actual) versus predicted values calculated according to the quadratic modelling for leaching in the presence of RBC-MIL composite

4.4. Evaluation of the Independent Factors' Dynamic Effects and Interactions on the Eluate Cu Concentration

The influence of the sorbent-to-soil mass ratio (x_1) and leaching time (x_2) on the leaching of Cu is visualized in Figure 4.7. The result obtained after modelling is called the predicated eluate Cu surface which was plotted as a function of two components that varied in the factorial phase of the design of the experiment ($-1 \leq xi \leq +1$). To visualize the influence of the composites, surface plot for soil + RBC-MIL variant of amendment is shown in Figure 4.7. As can be observed, there was a strong relationship between RBC-MIL to the soil mass ratio in relation to the elaute concentration of Cu. The RBC-MIL has a substantial impact on the immobilization of Cu, as seen in Figure 4.7, since the driving force increased as the sorbent to soil mass ratio rose. This implies that, most of Cu could rapidly get absorbed at the early stages of the leaching process. In this regard, the response surface analysis was carried out to pinpoint the best independent variables interactions and ratios values that resulted in minimum concentration of Cu in real contaminated soil effluent. All these observations suggested that the active surface sites of RBC on the composite, which was dominant

during leaching was the main driver for the immobilization of Cu.

At the end of the modelling, the minimum concentration of 0.2 mg L^{-1} was achieved at an RBC-MIL to soil mass ratio of 3% (which corresponds to the coded value of +1) and a leaching period of two days (which corresponds to the coded value of -1). According to the obtained results, it was suggested that combining RBC with highly active metal-based organic frameworks (RBC-MIL) is a viable technique for reducing the risk of PTE mobilization in polluted soils.

In order to assess the validity of the model, we carried out confirmation experiments at the point of optimized the response. The actual number fell within the 95 % prediction range (88.98–96.47 %), suggesting that the model correctly predicted the responses.

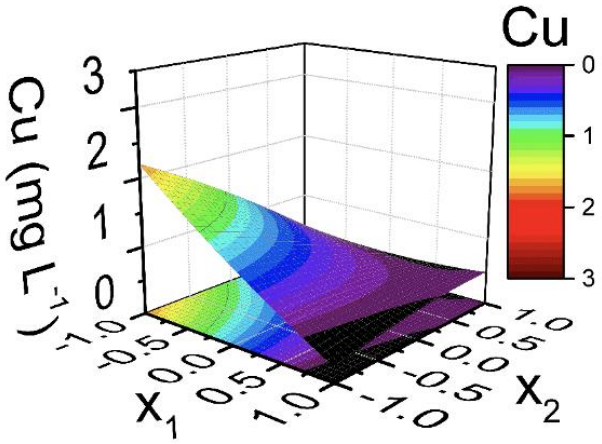

Figure 4.7. The three-dimensional response surface plots of Cu leachate (Y) as a function of the oindependent variables (x_1 and x_2) in the presence of RBC-MIL composite

4.5. Cu Fractionation Analysis

The sequential extraction method was used to assess the state of Cu distribution in different fractions of the amended soil after leaching process was completed. Figure 4.8. shows the proportion of four different fractions of Cu as explained in section 3.8. According to the fractionation results obtained before the commencement of the leaching experiment, the percentage of Cu in acid soluble, reducible, oxidable, and residual fractions were 20.6, 5.3, 9.5, and 64.6%, respectively. The observed high content of acid soluble is attributed to the presence of finely dispersed carbonates in the soil sample, as reported in the study by Minkina et al. (2016) (T. M. Minkina et al.,

2016). As a result of this phenomena, the components in the soil at this proportion are expected to be particularly accessible and transportable. The implication of the accesibility of Cu elements and it's potential to be transported under real field conditions is the overaching aim of this study. Hence, real field conditions that may likely affect the soil such as acidic rain, nitrogen addition fertilization, nitrogen-fixing plants should most be carefully assesed to curtail soil acidification, and metal leaching or transport (Puga, Melo, de Abreu, Coscione, & Paz-Ferreiro, 2016).

The distribution of Cu fractions in soil samples from different leaching days splitted into 2, 4, 6, and 8 days exhibited a similar tendency. The residual fraction accounted for the majority of Cu (69.6–79%), followed by acid soluble (15.6–6%), organic matter and sulfides (9.3–11%), and iron and manganese oxides (4.8–5.5%). As the amount of Cu linked to the residual fraction rose, the residual form of Cu began to dominate the leaching process (in increasing leaching time). This suggests that residual fraction of Cu had low potential toxicity. Also, the residual fraction of Cu could be increased due to the aging effect as a result of exchange reactions, chelation, and precipitation of metal ions on the surface of soil particle (B. Huang et al., 2015). The acid soluble fraction continued to decrease considerably in the presence of RBC-MIL amendments compared to each control group every leaching day. This observation might be explained by metal leaching behavior, as the reduction in the acid soluble percentage remaining in the soil resulted in a decrease in the mobility propensity of acid soluble fraction into leachate. The efficacy was acceptable after eight days, and the acid soluble percentage had decreased by 5.1 % to control soil on day 8. The oxidable fraction of Cu bound to organic matter and sulfur compounds showed insignificant changes compared to those in a group of controls on each day of the leaching process. Similarly, the reducible fraction of Cu bound to the fraction of iron-manganese oxides showed insignificant changes when compared to the control groups on the respective leaching days. With these observation in the oxidable and reducible fractions, It was suggested that neither an oxidative nor a reductive state existed during the leaching process.

During the leaching column experiment, RBC-MIL was discovered to reduce metal leaching. Notably, RBC-MIL significantly reduced the acid soluble fraction, according to chemical fractionation studies. Overall, the results of the sequential metal fractionation experiment were generally consistent with results obtained during the

column leaching experiment.

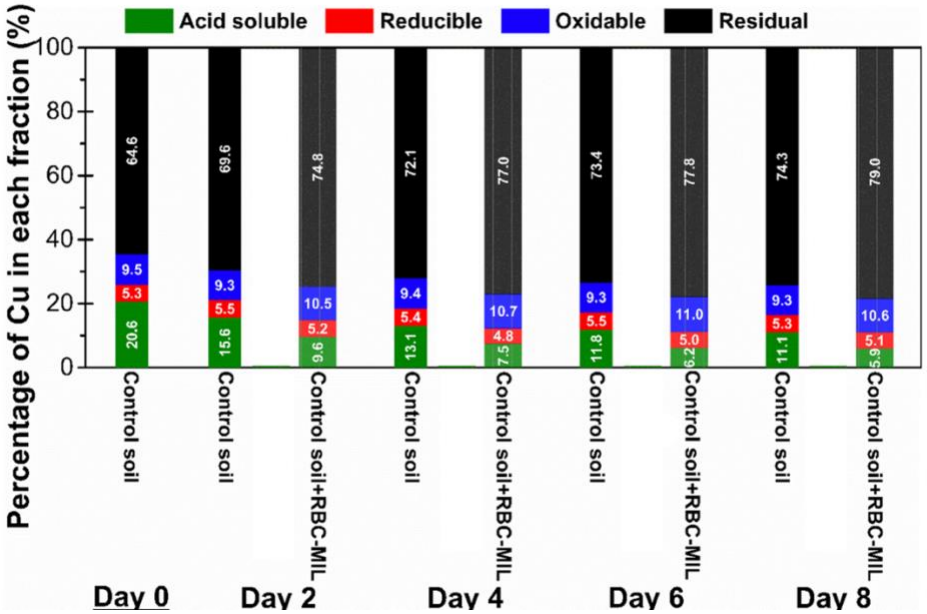

Figure 4.8. The percentages of Cu in each fraction of the soil samples withdraw from the leaching columns at control day and after 2, 4, 6, and 8 days in the presence of RBC-MIL at 3% sorbent to soil mass ratio

4.6. Proposed Mechanism

The mechanism driving the immobilization of Cu onto carbonaceous materials are well established. In accordance with previous studies by Merdy et al. (2009) and, Seco et al. (1997) (Merdy et al., 2009; Seco, Marzal, Gabaldón, & Ferrer, 1997), the adsorption affinity of PTEs onto carbonaceous material may be linked to the electronegativity of Cu, which was reported as the electrostatic interaction between Cu and biochar's surface. As a result, Cu might have adhered to the RBC-MIL surface and was subsequently removed from the Cu eluating solution. Electrostatic contact, ion exchange, and layer retention might all be responsible for Cu sorption by RBC-MIL based on the literature (Li et al., 2021b; S. Zhang et al., 2021b)

Aditionally, according to the the FTIR results of RBC-MIL, C–O–C, OH, C=C, and C–O functional groups appeared to improve the affinity between Cu and the composite. Hence, it is possible that the composite immobilized the free portion of Cu through surface complexation lowering Cu solubility. These findings are in close agreement with the previous studies on the adsorption of Cu by MOFs (Bakhtiari & Azizian, 2015; Ghaedi et al., 2018). In this study, we proposed a mechanism based on

cation exchange and complexation for the immobilization of Cu in the presence of RBC-MIL as illustrated in Figure 4.9.

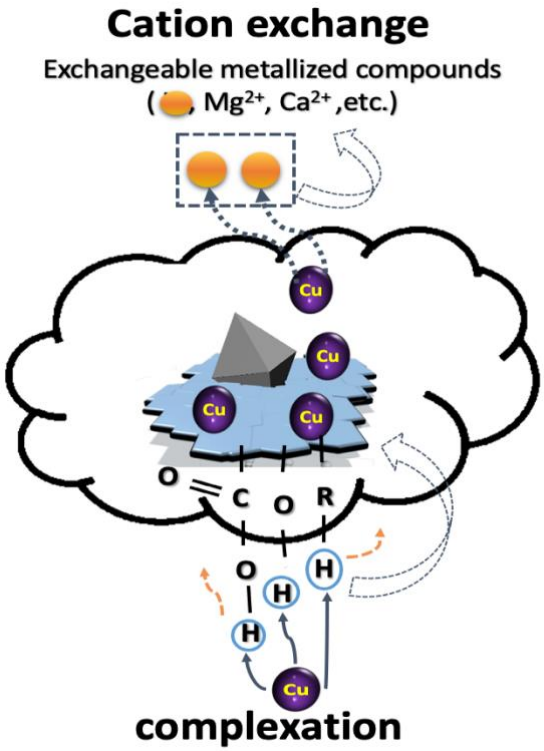

Figure 4.9. The proposed mechanism for Cu immobilization in the presence of RBC-MIL

5.CONCLUSION

In this study, MIL-101(Fe) decorated biochar (RBC-MIL) was synthesized to amend a real contaminated technogenic soil in a dynamic leaching experiment. In this context, the leachability of Cu was investigated, and the varied fraction contents of Cu were closely monitored.

The best optimized RBC-MIL composite was developed at the ratio of iron (III) chloride hexahydrate ($FeCl_3.6H_2O$) to 1,4-benzene dicarboxylic acid (H_2BDC) at 4.9 mmol to 2.48 mmol (2:1) with rice husk biochar (RBC) at 0.05g during the synthesis procedure.

The XRD patterns of composites confirmed the successful formation of a zeotype octahedral structure of MIL-101(Fe) on the surface of rice husk biochar (RBC). According to the FTIR results of RBC-MIL, C–O–C, OH, C=C, and C–O functional groups appeared to improve the affinity between Cu and the composite. The SEM and TEM characterization of the RBC-MIL manifested its porous zeotype octahedral forms.

The quadratic models were developed by fitting 3D surfaces on the obtained results from the dynamic leaching experiment. The response surface models were able to predict the leachate concentration of Cu with high precisions. After optimizations, it was found that 3% RBC-MIL to soil mass ratio and 2 days of leaching period resulted in the minimum Cu concentration of 0.2 mg L^{-1}.

Having investigated on the sequential fractionation of Cu after the leaching experiment, we conclude that acid soluble fraction dropped by 5.1% as compared to control soil. A rise in the residual fraction was also observed, suggesting that Cu availability was decreased significantly. The findings obtained from the sequential fractionation of metal were generally consistent with the results obtained during the column leaching experiment.

The mechanism driving the immobilization of the free portion of Cu was mainly through surface complexation and cation exchange interaction governed by the RBC-MIL composite.

These results suggested that using MIL decorated biochar could be a promising viable (effective, eco-friendly, and cheap) candidate for immobilizing the PTEs in real

technogenic soil especially during migration.

Beyond the scope of this study, for future studies, we recommend that a robust system should be employed to simulate a more realistic condition of precipitation with a bigger volume and at a bigger scale or automated leaching column arrangement. Addtionally, it will be of great significance to test the RSM model on other heavy metals to understand the different responses of the immobilization effects of the eluating solution.

REFERENCES

Ahmad, M., Rajapaksha, A. U., Lim, J. E., Zhang, M., Bolan, N., Mohan, D., … Ok, Y. S. (2014). Biochar as a sorbent for contaminant management in soil and water: A review. *Chemosphere*, 99, 19–33. Retrieved from https://doi.org/10.1016/j.chemosphere.2013.10.071

Anae, J., Ahmad, N., Kumar, V., Thakur, V. K., Gutierrez, T., Yang, X. J., … Coulon, F. (2021a). Recent advances in biochar engineering for soil contaminated with complex chemical mixtures: Remediation strategies and future perspectives. *Science of the Total Environment*, 767, 144351. Retrieved from https://doi.org/10.1016/j.scitotenv.2020.144351

Anae, J., Ahmad, N., Kumar, V., Thakur, V. K., Gutierrez, T., Yang, X. J., … Coulon, F. (2021b). Recent advances in biochar engineering for soil contaminated with complex chemical mixtures: Remediation strategies and future perspectives. *Science of The Total Environment*, 767, 144351. Retrieved from https://doi.org/10.1016/j.scitotenv.2020.144351

Arabyarmohammadi, H., Darban, A. K., Abdollahy, M., Yong, R., Ayati, B., Zirakjou, A., & van der Zee, S. E. A. T. M. (2018). Utilization of a Novel Chitosan/Clay/Biochar Nanobiocomposite for Immobilization of Heavy Metals in Acid Soil Environment. *Journal of Polymers and the Environment*, 26(5), 2107–2119. Retrieved from https://doi.org/10.1007/s10924-017-1102-6

Bakhtiari, N., & Azizian, S. (2015). Adsorption of copper ion from aqueous solution by nanoporous MOF-5: A kinetic and equilibrium study. *Journal of Molecular Liquids*, 206, 114–118. Retrieved from https://doi.org/10.1016/j.molliq.2015.02.009

Bano, A., Hussain, J., Akbar, A., Mehmood, K., Anwar, M., Hasni, M. S., … Ali, I. (2018). Biosorption of heavy metals by obligate halophilic fungi. *Chemosphere*, 199, 218–222. Retrieved from https://doi.org/10.1016/j.chemosphere.2018.02.043

Bashir, S., Hussain, Q., Shaaban, M., & Hu, H. (2018). Efficiency and surface characterization of different plant derived biochar for cadmium (Cd) mobility, bioaccessibility and bioavailability to Chinese cabbage in highly contaminated soil. *Chemosphere*, 211, 632–639. Retrieved from https://doi.org/10.1016/j.chemosphere.2018.07.168

Bayero, M. T., Mazarji, M., Sushkova, S., Minkina, T., Mandzhieva, S., Bauer, T., … Dengiz, O. (2021). Exploring the potential of metal-organic frameworks (MOFs) decorated biochar for the remediation of heavy metal-contaminated media (pp. 140–144). Samsun, Turkey: FESSS. Retrieved from http://www.fesss.org/pages.php?id=6

Beesley, L., & Marmiroli, M. (2011). The immobilisation and retention of soluble arsenic, cadmium and zinc by biochar. *Environmental Pollution*, 159(2), 474–480. Retrieved from https://doi.org/10.1016/j.envpol.2010.10.016

Beiyuan, J., Awad, Y. M., Beckers, F., Wang, J., Tsang, D. C. W., Ok, Y. S., … Rinklebe, J. (2020). (Im)mobilization and speciation of lead under dynamic redox conditions in a contaminated soil amended with pine sawdust biochar. *Environment International*, 135(September 2019), 105376. Retrieved from https://doi.org/10.1016/j.envint.2019.105376

Bian, R., Chen, D., Liu, X., Cui, L., Li, L., Pan, G., … Chang, A. (2013). Biochar soil amendment as a solution to prevent Cd-tainted rice from China: Results from a cross-site field experiment. *Ecological Engineering*, 58, 378–383. Retrieved from

https://doi.org/10.1016/j.ecoleng.2013.07.031
Black, C. A., Evans, D. D., & Dinauer, R. C. (1965). Methods of soil analysis.
Chausali, N., Saxena, J., & Prasad, R. (2021). Nanobiochar and biochar based nanocomposites: Advances and applications. *Journal of Agriculture and Food Research*, 5, 100191. Retrieved from https://doi.org/10.1016/j.jafr.2021.100191
Chen, D., Wang, X., Wang, X., Feng, K., Su, J., & Dong, J. (2020). The mechanism of cadmium sorption by sulphur-modified wheat straw biochar and its application cadmium-contaminated soil. *Science of the Total Environment*, 714, 136550. Retrieved from https://doi.org/10.1016/j.scitotenv.2020.136550
Chen, M., Wang, D., Xu, X., Zhang, Y., Gui, X., Song, B., & Xu, N. (2022). Biochar nanoparticles with different pyrolysis temperatures mediate cadmium transport in water-saturated soils: Effects of ionic strength and humic acid. *Science of the Total Environment*, 806, 150668. Retrieved from https://doi.org/10.1016/j.scitotenv.2021.150668
Fan, J., Chen, X., Xu, Z., Xu, X., Zhao, L., Qiu, H., & Cao, X. (2020a). One-pot synthesis of nZVI-embedded biochar for remediation of two mining arsenic-contaminated soils: Arsenic immobilization associated with iron transformation. *Journal of Hazardous Materials*, 398(May), 122901. Retrieved from https://doi.org/10.1016/j.jhazmat.2020.122901
Fan, J., Chen, X., Xu, Z., Xu, X., Zhao, L., Qiu, H., & Cao, X. (2020b). One-pot synthesis of nZVI-embedded biochar for remediation of two mining arsenic-contaminated soils: Arsenic immobilization associated with iron transformation. *Journal of Hazardous Materials*, 398(April), 122901. Retrieved from https://doi.org/10.1016/j.jhazmat.2020.122901
FAO. (2015). World reference base for soil resources Reports No. 106: International soil classification system for naming soils and creating legends for soil maps. *World Soil Resources Reports No. 106*. Roma: Fao Rome.
Ghaedi, A. M., Panahimehr, M., Nejad, A. R. S., Hosseini, S. J., Vafaei, A., & Baneshi, M. M. (2018). Factorial experimental design for the optimization of highly selective adsorption removal of lead and copper ions using metal organic framework MOF-2 (Cd). *Journal of Molecular Liquids*, 272, 15–26. Retrieved from https://doi.org/10.1016/j.molliq.2018.09.051
Gholizadeh, M., & Hu, X. (2021a). Removal of heavy metals from soil with biochar composite: A critical review of the mechanism. *Journal of Environmental Chemical Engineering*, 9(5), 105830. Retrieved from https://doi.org/10.1016/j.jece.2021.105830
Gholizadeh, M., & Hu, X. (2021b). Removal of heavy metals from soil with biochar composite: A critical review of the mechanism. *Journal of Environmental Chemical Engineering*, 9(5), 105830. Retrieved from https://doi.org/10.1016/j.jece.2021.105830
GOST 17.4.4.02–84. (2008). *Nature Protection. Methods of Sampling and Sample Preparation for Chemical, Bacteriological, and Helmintologic Analysis. Standardinform*. Retrieved from Moscow. (in Russian).:
Hanrahan, G., & Lu, K. (2006a). Application of Factorial and Response Surface Methodology in Modern Experimental Design and Optimization. *Critical Reviews in Analytical Chemistry*, 36(3–4), 141–151. Retrieved from https://doi.org/10.1080/10408340600969478
Hanrahan, G., & Lu, K. (2006b). Application of Factorial and Response Surface Methodology in Modern Experimental Design and Optimization. *Critical Reviews in Analytical Chemistry*, 36(3–4), 141–151. Retrieved from

https://doi.org/10.1080/10408340600969478
Hayyat, A., Javed, M., Rasheed, I., Ali, S., Shahid, M. J., Rizwan, M., … Ali, Q. (2016). *Role of Biochar in Remediating Heavy Metals in Soil. Chapter 14. In Phytoremediation.Management of Environmental Contaminants, Volume 3. Ed. Ali Abid, Sarvajeet Ansari, Gill Singh, Gill Ritu, Lanza Guy R* (Vol. 3).
Ho, S. H., Zhu, S., & Chang, J. S. (2017). Recent advances in nanoscale-metal assisted biochar derived from waste biomass used for heavy metals removal. *Bioresource Technology*, 246(June), 123–134. Retrieved from https://doi.org/10.1016/j.biortech.2017.08.061
Huang, B., Li, Z., Huang, J., Chen, G., Nie, X., Ma, W., … Zeng, G. (2015). Aging effect on the leaching behavior of heavy metals (Cu, Zn, and Cd) in red paddy soil. *Environmental Science and Pollution Research*, 22(15), 11467–11477. Retrieved from https://doi.org/10.1007/s11356-015-4386-x
Huang, D., Wang, G., Cheng, M., Zhang, G., Chen, S., Liu, Y., … Xiao, R. (2021). Optimal preparation of catalytic Metal-organic framework derivatives and their efficient application in advanced oxidation processes. *Chemical Engineering Journal*, 421(P2), 127817. Retrieved from https://doi.org/10.1016/j.cej.2020.127817
Huang, H., Reddy, N. G., Huang, X., Chen, P., Wang, P., Zhang, Y., … Garg, A. (2021). Effects of pyrolysis temperature, feedstock type and compaction on water retention of biochar amended soil. *Scientific Reports*, 11(1), 1–19. Retrieved from https://doi.org/10.1038/s41598-021-86701-5
Huang, J., Guo, S., Zeng, G. ming, Li, F., Gu, Y., Shi, Y., … Peng, S. (2018). A new exploration of health risk assessment quantification from sources of soil heavy metals under different land use. *Environmental Pollution*, 243, 49–58. Retrieved from https://doi.org/10.1016/j.envpol.2018.08.038
Irshad, M., & Mukhtar, S. O. (2020). Influence of selected mineral material on the water solubility and leachability of heavy metals from contaminated soil. *Arabian Journal of Geosciences*, 13(20). Retrieved from https://doi.org/10.1007/s12517-020-06114-y
ISO 10390. (2005). Soil quality — Determination of pH.
ISO 13317-2. (2001). Determination of particle size distribution by gravitational liquid sedimentation methods – Part 2: Fixed Pipette Method.
ISO 23470. (2018). Soil quality — Determination of effective cation exchange capacity (CEC) and exchangeable cations using a hexamminecobalt(III)chloride solution.
IUSS. (2014). *World Reference Base for Soil Resources. World Soil Resources Reports 106. World Soil Resources Reports No. 106*.
Jones, R. (2002). Design and Analysis of Experiments (fifth edition), Douglas Montgomery, John Wiley and Sons, 2001, 684 pages, £33.95. *Quality and Reliability Engineering International*, 18(2), 163. Retrieved from https://doi.org/10.1002/qre.458
Kim, S. O., Jeong, J. Y., Lee, W. C., Yun, S. T., & Jo, H. Y. (2021). Electrokinetic remediation of heavy metal-contaminated soils: performance comparison between one- and two-dimensional electrode configurations. *Journal of Soils and Sediments*, 21(8), 2755–2769. Retrieved from https://doi.org/10.1007/s11368-020-02803-z
Lado, L. R., Hengl, T., & Reuter, H. I. (2008). Heavy metals in European soils: A geostatistical analysis of the FOREGS Geochemical database. *Geoderma*, 148(2), 189–199. Retrieved from https://doi.org/10.1016/j.geoderma.2008.09.020

Li, Z., Wang, L., Qin, L., Lai, C., Wang, Z., Zhou, M., … Zhang, M. (2021a). Recent advances in the application of water-stable metal-organic frameworks: Adsorption and photocatalytic reduction of heavy metal in water. *Chemosphere*, 285(July), 131432. Retrieved from https://doi.org/10.1016/j.chemosphere.2021.131432

Li, Z., Wang, L., Qin, L., Lai, C., Wang, Z., Zhou, M., … Zhang, M. (2021b). Recent advances in the application of water-stable metal-organic frameworks: Adsorption and photocatalytic reduction of heavy metal in water. *Chemosphere*, 285(July), 131432. Retrieved from https://doi.org/10.1016/j.chemosphere.2021.131432

Liang, L., Xi, F., Tan, W., Meng, X., Hu, B., & Wang, X. (2021). Review of organic and inorganic pollutants removal by biochar and biochar-based composites. *Biochar*, 3(3), 255–281. Retrieved from https://doi.org/10.1007/s42773-021-00101-6

Linnik, V. G., Saveliev, A. A., Bauer, T. V., Minkina, T. M., & Mandzhieva, S. S. (2021). Analysis and assessment of heavy metal contamination in the vicinity of Lake Atamanskoe (Rostov region, Russia) using multivariate statistical methods. *Environmental Geochemistry and Health*, 0123456789. Retrieved from https://doi.org/10.1007/s10653-021-00853-x

Liu, J., Liu, Y. J., Liu, Y., Liu, Z., & Zhang, A. N. (2018). Quantitative contributions of the major sources of heavy metals in soils to ecosystem and human health risks: A case study of Yulin, China. *Ecotoxicology and Environmental Safety*, 164(June), 261–269. Retrieved from https://doi.org/10.1016/j.ecoenv.2018.08.030

Liu, S., Lai, C., Liu, X., Li, B., Zhang, C., Qin, L., … Chen, L. (2020). Metal-organic frameworks and their derivatives as signal amplification elements for electrochemical sensing. *Coordination Chemistry Reviews*, 424, 213520. Retrieved from https://doi.org/10.1016/j.ccr.2020.213520

Lu, H. P., Li, Z. A., Gascó, G., Méndez, A., Shen, Y., & Paz-Ferreiro, J. (2018). Use of magnetic biochars for the immobilization of heavy metals in a multi-contaminated soil. *Science of the Total Environment*, 622–623, 892–899. Retrieved from https://doi.org/10.1016/j.scitotenv.2017.12.056

Lyu, H., Zhao, H., Tang, J., Gong, Y., Huang, Y., Wu, Q., & Gao, B. (2018). Immobilization of hexavalent chromium in contaminated soils using biochar supported nanoscale iron sulfide composite. *Chemosphere*, 194, 360–369. Retrieved from https://doi.org/10.1016/j.chemosphere.2017.11.182

Mahmoodi, N. M., Oveisi, M., Panahdar, A., Hayati, B., & Nasiri, K. (2020a). Synthesis of porous metal-organic framework composite adsorbents and pollutant removal from multicomponent systems. *Materials Chemistry and Physics*, 243(September 2019), 122572. Retrieved from https://doi.org/10.1016/j.matchemphys.2019.122572

Mahmoodi, N. M., Oveisi, M., Panahdar, A., Hayati, B., & Nasiri, K. (2020b). Synthesis of porous metal-organic framework composite adsorbents and pollutant removal from multicomponent systems. *Materials Chemistry and Physics*, 243(September 2019), 122572. Retrieved from https://doi.org/10.1016/j.matchemphys.2019.122572

Mahmoodi, N. M., Taghizadeh, M., & Taghizadeh, A. (2019a). Activated carbon/metal-organic framework composite as a bio-based novel green adsorbent: Preparation and mathematical pollutant removal modeling. *Journal of Molecular Liquids*, 277, 310–322. Retrieved from

https://doi.org/10.1016/j.molliq.2018.12.050
Mahmoodi, N. M., Taghizadeh, M., & Taghizadeh, A. (2019b). Activated carbon/metal-organic framework composite as a bio-based novel green adsorbent: Preparation and mathematical pollutant removal modeling. *Journal of Molecular Liquids*, 277, 310–322. Retrieved from https://doi.org/10.1016/j.molliq.2018.12.050
Mandal, S., Pu, S., Adhikari, S., Ma, H., Kim, D. H., Bai, Y., & Hou, D. (2021). Progress and future prospects in biochar composites: Application and reflection in the soil environment. *Critical Reviews in Environmental Science and Technology*, 51(3), 219–271. Retrieved from https://doi.org/10.1080/10643389.2020.1713030
Mandal, S., Pu, S., He, L., Ma, H., & Hou, D. (2020a). Biochar induced modification of graphene oxide & nZVI and its impact on immobilization of toxic copper in soil. *Environmental Pollution*, 259, 113851. Retrieved from https://doi.org/10.1016/j.envpol.2019.113851
Mandal, S., Pu, S., He, L., Ma, H., & Hou, D. (2020b). Biochar induced modification of graphene oxide & nZVI and its impact on immobilization of toxic copper in soil. *Environmental Pollution*, 259, 113851. Retrieved from https://doi.org/10.1016/j.envpol.2019.113851
Mandal, S., Pu, S., Shangguan, L., Liu, S., Ma, H., Adhikari, S., & Hou, D. (2020). Synergistic construction of green tea biochar supported nZVI for immobilization of lead in soil: A mechanistic investigation. *Environment International*, 135(December 2019), 105374. Retrieved from https://doi.org/10.1016/j.envint.2019.105374
Mazarji, M., Bayero, M. T., Minkina, T., Sushkova, S., Mandzhieva, S., Tereshchenko, A., … Keswani, C. (2021). Realizing united nations sustainable development goals for greener remediation of heavy metals-contaminated soils by biochar: Emerging trends and future directions. *Sustainability (Switzerland)*, 13(24). Retrieved from https://doi.org/10.3390/su132413825
Mazarji, M., Minkina, T., Sushkova, S., Mandzhieva, S., Fedorenko, A., Bauer, T., … Dudnikova, T. (2022). Biochar-assisted Fenton-like oxidation of benzo[a]pyrene-contaminated soil. *Environmental Geochemistry and Health*, 44(1), 195–206. Retrieved from https://doi.org/10.1007/s10653-020-00801-1
Merdy, P., Gharbi, L. T., & Lucas, Y. (2009). Pb, Cu and Cr interactions with soil: Sorption experiments and modelling. *Colloids and Surfaces A: Physicochemical and Engineering Aspects*, 347(1–3), 192–199. Retrieved from https://doi.org/10.1016/j.colsurfa.2009.04.004
Minkina, T. M., Soldatov, A. V., Nevidomskaya, D. G., Motuzova, G. V., Podkovyrina, Y. S., & Mandzhieva, S. S. (2016). New approaches to studying heavy metals in soils by X-ray absorption spectroscopy (XANES)) and extractive fractionation. *Geochemistry International*, 54(2), 197–204. Retrieved from https://doi.org/10.1134/S001670291512006X
Minkina, T., Nevidomskaya, D., Shuvaeva, V., Bauer, T., Soldatov, A., Mandzhieva, S., … Ghazaryan, K. (2019). Molecular characterization of Zn in Technosols using X-ray absorption spectroscopy. *Applied Geochemistry*, 104(March), 168–175. Retrieved from https://doi.org/10.1016/j.apgeochem.2019.03.021
Moradi, S. E., Shabani, A. M. H., Dadfarnia, S., & Emami, S. (2016). Sulfonated metal organic framework loaded on iron oxide nanoparticles as a new sorbent for the magnetic solid phase extraction of cadmium from environmental water samples. *Analytical Methods*, 8(33), 6337–6346. Retrieved from

https://doi.org/10.1039/c6ay01692h
Muñoz-Senmache, J. C., Kim, S., Arrieta-Pérez, R. R., Park, C. M., Yoon, Y., & Hernández-Maldonado, A. J. (2020). Activated Carbon–Metal Organic Framework Composite for the Adsorption of Contaminants of Emerging Concern from Water. *ACS Applied Nano Materials*, 3(3), 2928–2940. Retrieved from https://doi.org/10.1021/acsanm.0c00190
Pachfule, P., Balan, B. K., Kurungot, S., & Banerjee, R. (2012). One-dimensional confinement of a nanosized metal organic framework in carbon nanofibers for improved gas adsorption. *Chemical Communications*, 48(14), 2009–2011. Retrieved from https://doi.org/10.1039/c2cc16877d
Puga, A. P., Melo, L. C. A., de Abreu, C. A., Coscione, A. R., & Paz-Ferreiro, J. (2016). Leaching and fractionation of heavy metals in mining soils amended with biochar. *Soil and Tillage Research*, 164, 25–33. Retrieved from https://doi.org/10.1016/j.still.2016.01.008
Qian, W., Liang, J. Y., Zhang, W. X., Huang, S. T., & Diao, Z. H. (2022a). A porous biochar supported nanoscale zero-valent iron material highly efficient for the simultaneous remediation of cadmium and lead contaminated soil. *Journal of Environmental Sciences (China)*, 113, 231–241. Retrieved from https://doi.org/10.1016/j.jes.2021.06.014
Qian, W., Liang, J. Y., Zhang, W. X., Huang, S. T., & Diao, Z. H. (2022b). A porous biochar supported nanoscale zero-valent iron material highly efficient for the simultaneous remediation of cadmium and lead contaminated soil. *Journal of Environmental Sciences (China)*, 113, 231–241. Retrieved from https://doi.org/10.1016/j.jes.2021.06.014
Saedi, Z., Tangestaninejad, S., Moghadam, M., Mirkhani, V., & Mohammadpoor-Baltork, I. (2012). The effect of encapsulated Zn-POM on the catalytic activity of MIL-101 in the oxidation of alkenes with hydrogen peroxide. *Journal of Coordination Chemistry*, 65(3), 463–473. Retrieved from https://doi.org/10.1080/00958972.2011.648929
Sarwar, N., Imran, M., Shaheen, M. R., Ishaque, W., Kamran, M. A., Matloob, A., … Hussain, S. (2017). Phytoremediation strategies for soils contaminated with heavy metals: Modifications and future perspectives. *Chemosphere*, 171, 710–721. Retrieved from https://doi.org/10.1016/j.chemosphere.2016.12.116
Seco, A., Marzal, P., Gabaldón, C., & Ferrer, J. (1997). Adsorption of heavy metals from aqueous solutions onto activated carbon in single Cu and Ni systems and in binary Cu-Ni, Cu-Cd and Cu-Zn systems. *Journal of Chemical Technology and Biotechnology*, 68(1), 23–30. Retrieved from https://doi.org/10.1002/(SICI)1097-4660(199701)68:1<23::AID-JCTB595>3.0.CO;2-N
Sun, D. T., Peng, L., Reeder, W. S., Moosavi, S. M., Tiana, D., Britt, D. K., … Queen, W. L. (2018). Rapid, Selective Heavy Metal Removal from Water by a Metal-Organic Framework/Polydopamine Composite. *ACS Central Science*, 4(3), 349–356. Retrieved from https://doi.org/10.1021/acscentsci.7b00605
Tessier, A., Campbell, P. G. C., & Bisson, M. (1979). Sequential Extraction Procedure for the Speciation of Particulate Trace Metals. *Analytical Chemistry*, 51(7), 844–851. Retrieved from https://doi.org/10.1021/ac50043a017
Wan, X., Lei, M., & Chen, T. (2016). Cost–benefit calculation of phytoremediation technology for heavy-metal-contaminated soil. *Science of the Total Environment*, 563–564, 796–802. Retrieved from https://doi.org/10.1016/j.scitotenv.2015.12.080

Wang, Y., Guo, W., & Li, X. (2018). Activation of persulfates by ferrocene-MIL-101(Fe) heterogeneous catalyst for degradation of bisphenol A. *RSC Advances*, 8(64), 36477–36483. Retrieved from https://doi.org/10.1039/C8RA07007E

Wei, N., Zheng, X., Ou, H., Yu, P., Li, Q., & Feng, S. (2019). Fabrication of an amine-modified ZIF-8@GO membrane for high-efficiency adsorption of copper ions. *New Journal of Chemistry*, 43(14), 5603–5610. Retrieved from https://doi.org/10.1039/C8NJ06521G

Wu, P., Wang, Z., Wang, H., Bolan, N. S., Wang, Y., & Chen, W. (2020). Visualizing the emerging trends of biochar research and applications in 2019: a scientometric analysis and review. *Biochar*, 2(2), 135–150. Retrieved from https://doi.org/10.1007/s42773-020-00055-1

Xie, Q., Li, Y., Lv, Z., Zhou, H., Yang, X., Chen, J., & Guo, H. (2017). Effective Adsorption and Removal of Phosphate from Aqueous Solutions and Eutrophic Water by Fe-based MOFs of MIL-101. *Scientific Reports*, 7(1), 1–15. Retrieved from https://doi.org/10.1038/s41598-017-03526-x

Xie, T., Reddy, K. R., Wang, C., Yargicoglu, E., & Spokas, K. (2015). Characteristics and applications of biochar for environmental remediation: A review. *Critical Reviews in Environmental Science and Technology*, 45(9), 939–969. Retrieved from https://doi.org/10.1080/10643389.2014.924180

Yaashikaa, P. R., Kumar, P. S., Varjani, S., & Saravanan, A. (2020). A critical review on the biochar production techniques, characterization, stability and applications for circular bioeconomy. *Biotechnology Reports*, 28, e00570. Retrieved from https://doi.org/10.1016/j.btre.2020.e00570

Yu, Z., Zhou, L., Huang, Y., Song, Z., & Qiu, W. (2015). Effects of a manganese oxide-modified biochar composite on adsorption of arsenic in red soil. *Journal of Environmental Management*. Retrieved from https://doi.org/10.1016/j.jenvman.2015.08.020

Yutong, Z., Qing, X., & Shenggao, L. (2016). Chemical fraction, leachability, and bioaccessibility of heavy metals in contaminated soils, Northeast China. *Environmental Science and Pollution Research*, 23(23), 24107–24114. Retrieved from https://doi.org/10.1007/s11356-016-7598-9

Zhang, C., Qin, N., Li, J., Tian, Y., Zhang, H., & Ying, Y. (2019). Facile Synthesis of Fe Nanomaterials from MIL-101(Fe) Template and Its Application in Lithium Ion Batteries. *Journal of Nanomaterials*, 2019. Retrieved from https://doi.org/10.1155/2019/3108742

Zhang, S., Wang, J., Zhang, Y., Ma, J., Huang, L., Yu, S., … Wang, X. (2021a). Applications of water-stable metal-organic frameworks in the removal of water pollutants: A review. *Environmental Pollution*, 291(August), 118076. Retrieved from https://doi.org/10.1016/j.envpol.2021.118076

Zhang, S., Wang, J., Zhang, Y., Ma, J., Huang, L., Yu, S., … Wang, X. (2021b). Applications of water-stable metal-organic frameworks in the removal of water pollutants: A review. *Environmental Pollution*, 291(August), 118076. Retrieved from https://doi.org/10.1016/j.envpol.2021.118076

Zhao, C., Wang, B., Theng, B. K. G., Wu, P., Liu, F., Wang, S., … Zhang, X. (2021). Formation and mechanisms of nano-metal oxide-biochar composites for pollutants removal: A review. *Science of the Total Environment*, 767, 145305. Retrieved from https://doi.org/10.1016/j.scitotenv.2021.145305

CURRICULUM VITAE

Bachelor of Engineering (B.Eng.) in Water Resources and Environmental Engineering, Ahmadu Bello University, Zaria, Nigeria (2010-2015). Master of Science (M.Sc.) in Water Engineering, Pan African University Institute of Water and Energy Sciences (including Climate Change) (2017-2019).

Contact Information :

ORCID ID : 0000-0001-9663-3133

Publications :

1. Mahmoud Mazarji, Muhammad Tukur Bayero, Tatiana Minkina, Svetlana, Sushkova, Saglara Mandzhieva, Andrey Tereshchenko, Anna Timofeeva, Tatiana, Bauer, Marina Burachevskaya, Rıdvan Kızılkaya, Coskun Gulser, Chetan Keswani. "*Realizing United Nations Sustainable Development Goals for Greener Remediation of Heavy Metals-Contaminated Soils by Biochar: Emerging Trends and Future Directions.*" Sustainability 2021, 13(24), 13825. https://doi.org/10.3390/su132413825
2. Muhammad Tukur Bayero, Mahmoud Mazarji, Svetlana, Sushkova, Tatiana Minkina, Saglara Mandzhieva, Tatiana, Bauer, Coskun Gulser, Rıdvan Kızılkaya, Orhan Dengiz. (2021, December 18 -19). *Exploring the potential of metal-organic frameworks (MOFs) decorated biochar for the remediation of heavy metal-contaminated media* [paper Presentation]. International Soil Science Symposium on "SOIL SCIENCE & PLANT NUTRITION, Samsun, Turkey. http://www.fesss.org/pages.php?id=6
3. Muhammad Tukur Bayero, Mahmoud Mazarji, Tatiana Bauer, Svetlana Sushkova, Saglara Mandzhieva. (2022, March 1 - 3). *Towards the application of metal-organic framework for removal of heavy metal ions* [paper Presentation]. International scientific conference XXV Dokuchaev conference for young scientists: SOIL IS LIFE, St. Petersburg, Russia. http://www.dokuchaevskie.ru
4. Muhammad Tukur Bayero, Mahmoud Mazarji, Tatiana Bauer, Tatiana Minkina, Svetlana Sushkova, Saglara Mandzhieva, Anna Timofeeva, Rıdvan Kızılkaya, and Coşkun Gülser. (2022, May 23 - 27). *Biochar and metal-organic framework nanocomposite: Application for immobilization of Cu in polluted industrial soil* [paper Presentation]. EGU General Assembly, Vienna, Austria. EGU22-10121. https://www.egu22.eu/

Won Awards, Incentives and Scholarships

1. Erasmus Mundus Joint Master Degree Fellowship – Erasmus Mundus Master in Soil Science (emiSS) (2020-2022).